INDUCTORLESS BANDPASS FILTER REALIZATION USING THE RIORDAN GYRATOR

Robert Edward Mollet

United States
Naval Postgraduate School

THESIS

INDUCTORLESS BANDPASS FILTER REALIZATION
USING THE RIORDAN GYRATOR

by

Robert Edward Mollet

Thesis Advisor: S. R. Parker

September 1971

Inductorless Bandpass Filter Realization Using the Riordan Gyrator

by

Robert Edward Mollet
Lieutenant, United States Navy
B.S.E.E., Purdue University, 1966

Submitted in partial fulfillment of the
requirements for the degree of

MASTER OF SCIENCE IN ELECTRICAL ENGINEERING

from the

NAVAL POSTGRADUATE SCHOOL
September 1971

ABSTRACT

Since the gyrator was introduced over twenty years ago, a considerable number of realizations of the gyrator circuit have appeared in the technical literature. This thesis is confined to the study of only one of these, namely the Riordan gyrator circuit. The scope of the thesis is to analyze the parameters of the Riordan gyrator and those of an inductor simulated using it, and to investigate the use of simulated inductors in electric filter networks. To illustrate and support the theory surrounding the Riordan gyrator, an inductorless bandpass filter is designed, constructed, and tested.

TABLE OF CONTENTS

LIST OF TABLES

LIST OF ILLUSTRATIONS

I. THE RIORDAN GYRATOR

A. INTRODUCTION

Since the introduction of the gyrator in 1948 by Tellegen [1] a profusion of information concerning the gyrator has come forth in the technical literature. A great many realizations of the gyrator, including vacuum tube, transistor, and integrated circuit models, have appeared to date. Reference [2] has consolidated a considerable amount of information on gyrators.

The unique feature of the gyrator as a circuit element is its violation of the reciprocal behavior found in normal circuit elements. The circuit symbol for the ideal gyrator is shown in Fig. 1.1.

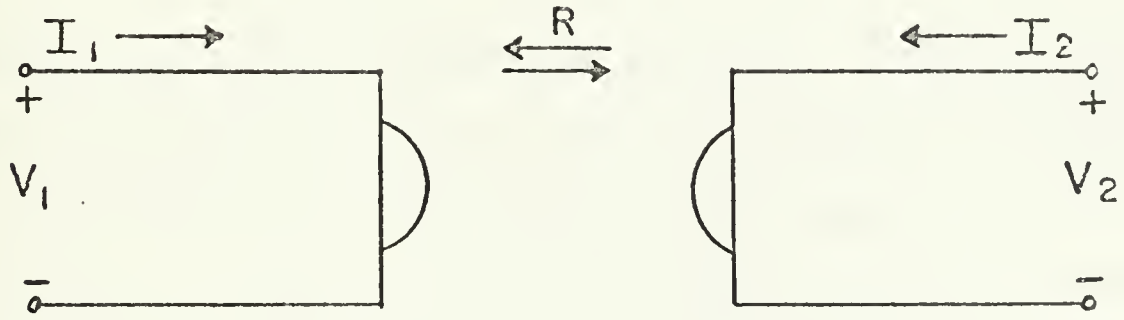

Figure 1.1. The Ideal Gyrator

The impedance matrix associated with the ideal gyrator is

$$[z] = \begin{bmatrix} 0 & \mp R \\ \pm R & 0 \end{bmatrix} , \qquad (1\text{-}1)$$

where R is referred to as the gyration resistance. Note that the input and output impedance of this two-port are zero, and the transfer impedances are equal in magnitude but opposite in sign. It is the latter characteristic of the gyrator that distinguishes it by violating the reciprocity theorem.

Since the input impedance Z_{in} of a two-port network loaded by an impedance Z_L is given by

$$Z_{in} = z_{11} - z_{12}z_{21}/(z_{22}+Z_L) , \qquad (1\text{-}2)$$

then for an ideal gyrator, Eq. (1-2) becomes

$$Z_{in} = R^2/Z_L . \qquad (1\text{-}3)$$

Therefore if a capacitor C is connected across the output port of an ideal gyrator, the input impedance is given by

$$Z_{in}(s) = sR^2C , \qquad (1\text{-}4)$$

which represents an inductor of value R^2C. Thus a gyrator loaded by a capacitor may be used to simulate an inductor. It is this feature of the gyrator which makes it an extremely valuable tool in the synthesis of inductorless LC filters, replacing relatively large physical inductors by high-Q, small-sized equivalent inductors.

One of the most promising gyrator circuits seems to be that which was proposed by Riordan [3] in 1966. Instead of

realizing a gyrator through the use of current sources as did many others, Riordan used a pair of operational amplifiers operated in the differential mode.

B. DERIVATION OF IMPEDANCE PARAMETERS

The gyrator circuit proposed by Riordan is shown in Fig. 1.2. Actually, the behavior of the circuit is essentially the same if the terminals 3-3' are taken as the output port and the resistor R_2 is shifted to terminals 2-2'; however, only the first circuit will be investigated, as the two are nearly identical.

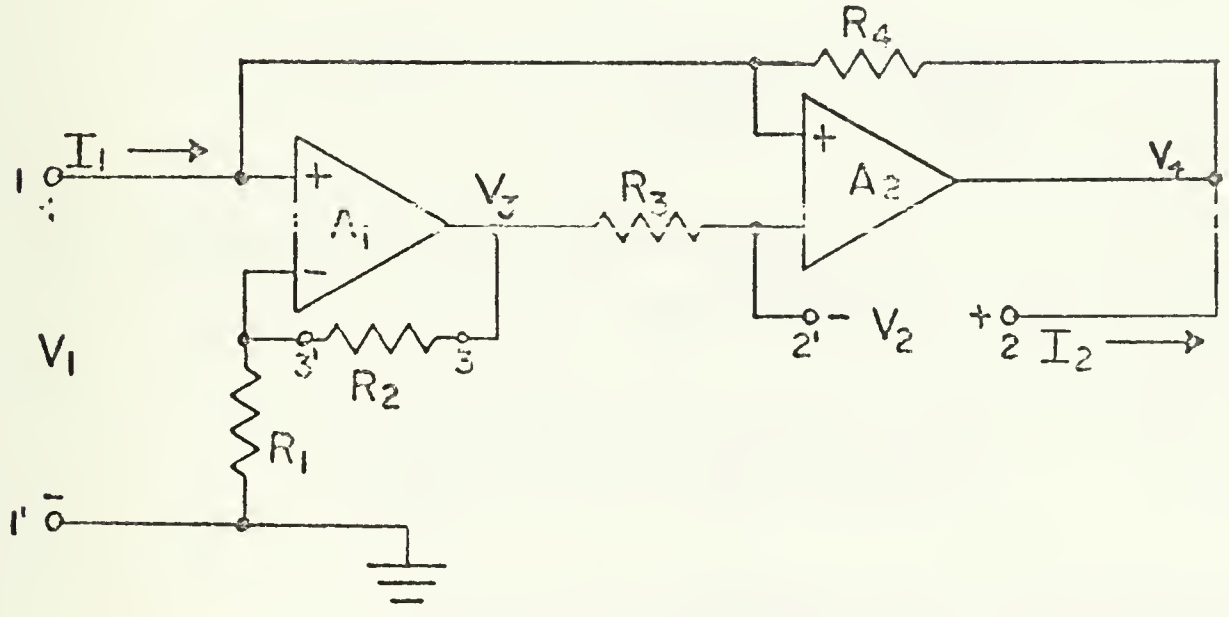

Figure 1.2. The Riordan Gyrator.

The following analysis of the Riordan Gyrator circuit assumes the operational amplifiers have infinite input impedances, zero output impedances, and finite gains.

When a current I_1 is injected into the input port with the output port open, the following equations result.

$$V_3 = \frac{A_1 V_1}{1 + \frac{A_1 R_1}{R_1+R_2}} \tag{1-5}$$

$$V_5 = V_3 \tag{1-6}$$

$$V_4 = -A_2 V_3 + A_2 V_1 = V_1 \left(A_2 - \frac{A_1 A_2}{1 + \frac{A_1 R_1}{R_1+R_2}}\right) \tag{1-7}$$

$$I_1 = \frac{V_1 - V_4}{R_4} = \frac{V_1}{R_4} \left(1 - A_2 + \frac{A_1 A_2}{1 + \frac{A_1 R_1}{R_1+R_2}}\right) \tag{1-8}$$

$$V_2 = V_4 - V_5 = V_4 - V_3$$

$$= V_1 \left(A_2 - \frac{A_1 A_2}{1 + \frac{A_1 R_1}{R_1+R_2}} - \frac{A_1}{1 + \frac{A_1 R_1}{R_1+R_2}}\right) \tag{1-9}$$

$$Z_{11} = \frac{V_1}{I_1}\Big|_{I_2=0} = \frac{R_4}{1 - A_2 + \frac{A_1 A_2}{1+A_1 R_1/(R_1+R_2)}}$$

$$= \frac{R_4 [1+A_1 R_1/(R_1+R_2)]}{A_1 A_2 + (1-A_2)[1+A_1 R_1/(R_1+R_2)]} \tag{1-10}$$

$$Z_{21} = \frac{V_2}{I_1}\Big|_{I_2=0} = \frac{R_4 \left[A_2 - \frac{A_1 A_2}{1+A_1 R_1/(R_1+R_2)} - \frac{A_1}{1+A_1 R_1/(R_1+R_2)}\right]}{1 - A_2 + \frac{A_1 A_2}{1+A_1 R_1/(R_1+R_2)}}$$

$$= \frac{R_4 \{-A_1 A_2 - A_1 + A_2 [1+A_1 R_1/(R_1+R_2)]\}}{A_1 A_2 + (1-A_2)[1+A_1 R_1/(R_1+R_2)]} \tag{1-11}$$

Now when a current I_2 is injected into the output port with the input port open, the following equations result.

$$V_1 = V_4 \tag{1-12}$$

$$V_3 = \frac{A_1 V_1}{1+A_1 R_1/(R_1+R_2)} = \frac{A_1 V_4}{1+A_1 R_1/(R_1+R_2)} \tag{1-13}$$

$$V_5 = V_3 - I_2 R_3 = \frac{A_1 V_4}{1+A_1 R_1/(R_1+R_2)} - I_2 R_3 \tag{1-14}$$

$$V_4 = -A_2 V_5 + A_2 V_1 = -A_2 V_5 + A_2 V_4 \tag{1-15}$$

$$V_5 = \frac{V_4 (A_2-1)}{A_2} = \frac{A_1 V_4}{1+A_1 R_1/(R_1+R_2)} - I_2 R_3 \tag{1-16}$$

$$V_4 = \frac{I_2 R_3}{\frac{A_1}{1+A_1 R_1/(R_1+R_2)} + \frac{1-A_2}{A_2}} \tag{1-17}$$

$$V_2 = V_4 - V_5 = V_4 [1-(A_2-1)/A_2] = \frac{V_4}{A_2}$$

$$= \frac{I_2 R_3}{\frac{A_1 A_2}{1+A_1 R_1/(R_1+R_2)} + 1 - A_2} \tag{1-18}$$

$$Z_{12} = \frac{V_1}{I_2}\Big|_{I_1=0} = \frac{R_3}{\frac{A_1}{1+A_1 R_1/(R_1+R_2)} + \frac{1-A_2}{A_2}}$$

$$= \frac{A_2 R_3 [1+A_1 R_1/(R_1+R_2)]}{A_1 A_2 + (1-A_2)[1+A_1 R_1/(R_1+R_2)]} \tag{1-19}$$

$$Z_{22} = \frac{V_2}{I_2}\Big|_{I_1=0} = \frac{R_3}{\frac{A_1 A_2}{1+A_1 R_1/(R_1+R_2)} + 1 - A_2}$$

$$= \frac{R_3 [1+A_1 R_1/(R_1+R_2)]}{A_1 A_2 + (1-A_2)[1+A_1 R_1/(R_1+R_2)]} \tag{1-20}$$

If $R_1 = R_2$, the open-circuit impedance parameters become:

$$z_{11} = \frac{R_4(1+A_1/2)}{A_1A_2+(1-A_2)(1+A_1/2)} = \frac{R_4(A_1+2)}{A_1A_2+A_1-2A_2+2} \qquad (1\text{-}21)$$

$$z_{12} = \frac{A_2R_3(1+A_1/2)}{A_1A_2+(1-A_2)(1+A_1/2)} = \frac{A_2R_3(A_1+2)}{A_1A_2+A_1-2A_2+2} \qquad (1\text{-}22)$$

$$z_{21} = \frac{R_4[-A_1A_2-A_1+A_2(1+A_1/2)]}{A_1A_2+(1-A_2)(1+A_1/2)} = \frac{-R_4(A_1A_2+2A_1-2A_2)}{A_1A_2+A_1-2A_2+2} \qquad (1\text{-}23)$$

$$z_{22} = \frac{R_3(1+A_1/2)}{A_1A_2+(1-A_2)(1+A_1/2)} = \frac{R_3(A_1+2)}{A_1A_2+A_1-2A_2+2} \; . \qquad (1\text{-}24)$$

These results are in agreement with those of Antoniou (4) in his paper on the Riordan gyrator, with the exceptions of notational differences and an extra denominator term in his equations for the impedance parameters (the latter difference undoubtedly attributed to his typist). Note that as the amplifier gains approach infinity, and if $R_3 = R_4 = R$, the impedance matrix becomes

$$[z] = \begin{bmatrix} 0 & R \\ -R & 0 \end{bmatrix} \; , \qquad (1\text{-}25)$$

which is that of an ideal gyrator.

C. SIMPLIFIED ANALYSIS OF CAPACITIVELY LOADED GYRATOR

If one assumes very large amplifier gains, the open-circuit impedance matrix for the Riordan gyrator may be approximated by

$$[z] = \begin{bmatrix} R_4/A_2 & R_3 \\ -R_4 & R_3/A_2 \end{bmatrix} \; . \qquad (1\text{-}26)$$

Now if a capacitor C is connected across the gyrator output port, the input impedance is computed as follows.

$$Z_{in}(s) = Z_{11} - Z_{12}Z_{21}/(Z_{22}+Z_L) = \frac{R_4}{A_2} + R_3R_4/(R_3/A_2+1/sC)$$

$$= \frac{R_4}{A_2} + \frac{sR_3R_4CA_2}{A_2+sR_3C} \qquad (1\text{-}27)$$

The amplifier gain is given by

$$A_2(s) = A_{20}\omega_c/(s+\omega_c) \ , \qquad (1\text{-}28)$$

where A_{20} is the DC open-loop gain and ω_c is the 3-db frequency. Therefore,

$$1/A_2(s) = (s+\omega_c)/A_{20}\omega_c = a(s+\omega_c)/\omega_c \qquad (1\text{-}29)$$

where $a = 1/A_{20}$.

The input impedance now becomes

$$Z_{in}(s) = a\ R_4(s+\omega_c)/\omega_c + R_3R_4/[a\ R_3(s+\omega_c)/\omega_c + 1/sC]$$

$$= a\ R_4(s+\omega_c)/\omega_c + sR_3R_4C/[1+asR_3C(s+\omega_c)/\omega_c]$$

$$= a\ R_4(s+\omega_c)/\omega_c + sR_3R_4C/(1+as^2R_3C/\omega_c+asR_3C) \ . \qquad (1\text{-}30)$$

$$Z_{in}(j\omega) = a\ R_4(j\omega+\omega_c)/\omega_c + j\omega R_3R_4C/(1-a\omega^2R_3C/\omega_c+j\omega aR_3C)$$

$$= j\omega aR_4/\omega_c + a\ R_4 + \frac{j\omega R_3R_4C(1-a\omega^2R_3C/\omega_c - j\omega aR_3C)}{(1-a\omega^2R_3C/\omega_c)^2 + (a\omega R_3C)^2}$$

$$\doteq j\omega aR_4/\omega_c + a\ R_4 + \frac{j\omega R_3R_4C(1-a\omega^2R_3C/\omega_c - j\omega aR_3C)}{1-2a\omega^2R_3C/\omega_c}$$

$$\doteq j\omega aR_4/\omega_c + a\ R_4$$
$$+ j\omega R_3R_4C(1-a\omega^2R_3C/\omega_c - j\omega aR_3C)(1+2a\omega^2R_3C/\omega_c)$$

$$\doteq j\omega aR_4/\omega_c + a\ R_4 + j\omega R_3R_4C(1+a\omega^2R_3C/\omega_c - j\omega aR_3C)$$

$$= j\omega R_3R_4C(1+a\omega^2R_3C/\omega_c + a/R_3C\omega_c)$$
$$+ a\omega R_3R_4C(\omega R_3C + 1/\omega R_3C)\ . \qquad (1\text{-}31)$$

Now the input impedance is of the form

$$Z_{in}(j\omega) = j\omega L_{eq} + R_{eq} \qquad (1\text{-}32)$$

Therefore,

$$L_{eq} = R_3R_4C(1+a\omega^2R_3C/\omega_c + a/R_3C\omega_c)$$

$$= R_3R_4C\left[1+\frac{a\omega}{\omega_c}\left(\omega R_3C+\frac{1}{\omega R_3C}\right)\right] \qquad (1\text{-}33)$$

$$R_{eq} = a\omega R_3R_4C(\omega R_3C + 1/\omega R_3C) \qquad (1\text{-}34)$$

$$D = \frac{1}{Q} = \frac{R_{eq}}{\omega L_{eq}} = \frac{a(\omega R_3 C + 1/\omega R_3 C)}{1 + a\omega^2 R_3 C/\omega_c + a/R_3 C\omega_c} \doteq a(\omega R_3 C + 1/\omega R_3 C) \qquad (1\text{-}35)$$

Inspection of Eq. (1-35), the expression for the dissipation factor, reveals that the term in brackets has a minimum value of two when the quantity $\omega R_3 C$ is unity, implying a maximum Q-factor for the Riordan-derived inductor of one-half the amplifier gain. The inductor produced has a value very close to that from an ideal gyrator when $R_3 = R_4 = R$, the gyration resistance. However, a closer analysis of the Riordan circuit in the following section will reveal a significantly different conclusion regarding the dissipation factor.

D. DETAILED ANALYSIS OF CAPACITIVELY LOADED GYRATOR

A more precise analysis of the capacitively loaded gyrator must include the effects of capacitance from the inputs of the operational amplifiers to ground. These capacitances are represented by C_1 and C_2 in Fig. 1.3, and include the naturally-occurring capacitance associated with each operational amplifier, plus an amount of capacitance inserted deliberately for Q-control. The latter effect will be demonstrated in the following analysis.

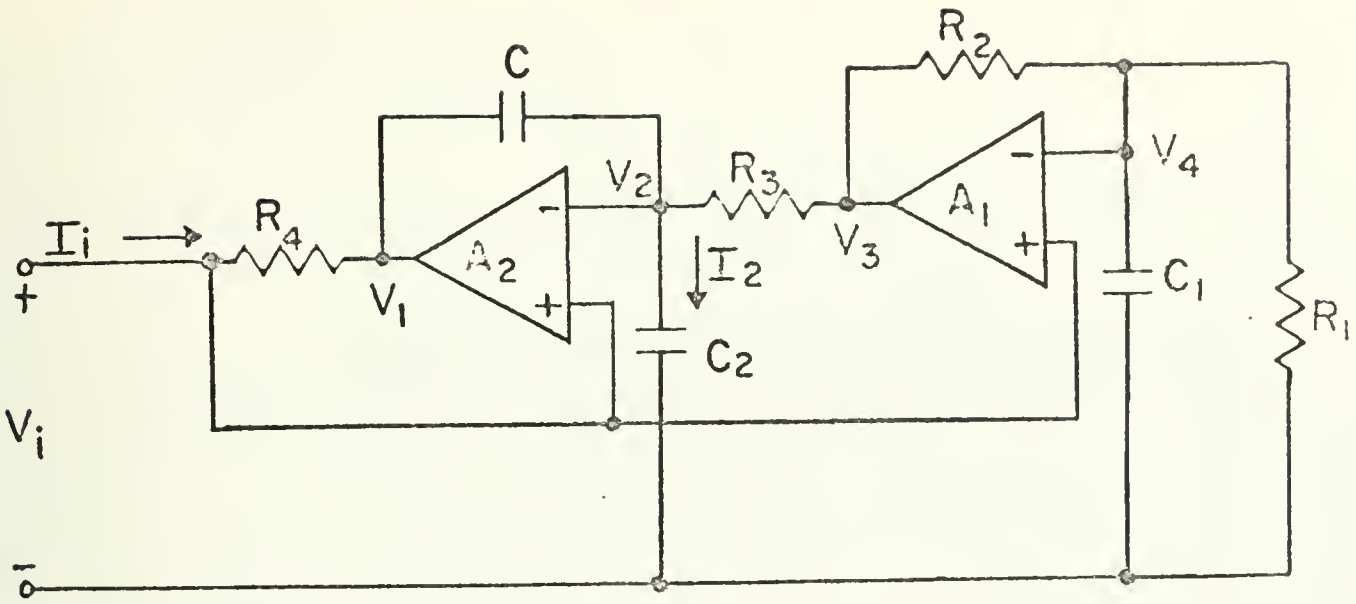

Figure 1.3. The Riordan Gyrator.

In the following analysis, the operational amplifiers are assumed to have infinite input impedances, zero output impedances, and large but finite gains.

$$V_3 = \frac{A_1 V_i}{1+A_1[(R_1/sC_1)/(R_1+1/sC_1)]/[R_2+(R_1/sC_1)/(R_1+1/sC_1)]}$$

$$= \frac{A_1 V_i}{1+A_1[R_1/(1+sR_1C_1)]/[R_2+R_1/(1+sR_1C_1)]}$$

$$= \frac{A_1 V_i}{1+A_1 R_1/[R_1+R_2(1+sR_1C_1)]} \qquad (1\text{-}36)$$

$$V_1 = A_2(V_i - V_2) \qquad (1\text{-}37)$$

$$I_2 = sC_2V_2 = (V_1-V_2)sC - (V_2-V_3)/R_3 \qquad (1\text{-}38)$$

$$V_2(sC_2+sC+1/R_3) = sCV_1 + V_3/R_3 \qquad (1\text{-}39)$$

$$V_2 = (sCV_1+V_3/R_3)/[s(C+C_2)+1/R_3] \tag{1-40}$$

$$V_1 = A_2\{V_i - (sCV_1+V_3/R_3)/[s(C+C_2)+1/R_3]\}$$

$$= A_2\left[V_i - \frac{sCV_1+(A_1V_i/R_3)/\{1+A_1R_1/[R_1+R_2(1+sR_1C_1)]\}}{s(C+C_2) + 1/R_3}\right] \tag{1-41}$$

$$V_1\{1+sCA_2/[s(C+C_2)+1/R_3]\}$$

$$= A_2V_i\left[1 - \frac{(A_1/R_3)/\{1+A_1R_1/[R_1+R_2(1+sR_1C_1)]\}}{s(C+C_2) + 1/R_3}\right] \tag{1-42}$$

$$V_1 = \frac{A_2V_i\left[1 - \frac{(A_1/R_3)/\{1+A_1R_1/[R_1+R_2(1+sR_1C_1)]\}}{s(C+C_2) + 1/R_3}\right]}{1+sCA_2/[s(C+C_2) + 1/R_3]}$$

$$= \frac{A_2V_i[s(C+C_2)+1/R_3-(A_1/R_3)/\{1+A_1R_1/[R_1+R_2(1+sR_1C_1)]\}]}{s(C+C_2) + 1/R_3 + sCA_2}$$

$$= \frac{A_2V_i\left\{sR_3(C+C_2)+1 - \frac{A_1[R_1+R_2(1+sR_1C_1)]}{R_1(1+A_1)+R_2(1+sR_1C_1)}\right\}}{1 + sR_3[C(1+A_2) + C_2]} \tag{1-43}$$

$$Z_i(s) = \frac{V_i}{I_i} = \frac{V_i}{(V_i-V_1)/R_4} = \frac{R_4}{1-V_1/V_i}$$

$$= \frac{R_4}{1-A_2\left\{1+sR_3(C+C_2)-\dfrac{A_1[R_1+R_2(1+sR_1C_1)]}{R_1(1+A_1)+R_2(1+sR_1C_1)}\right\}\dfrac{}{1+sR_3[C(1+A_2)+C_2]}}$$

$$= \frac{R_4\{1+sR_3[C(1+A_2)+C_2]\}}{1+sR_3[C(1+A_2)+C_2]}$$

$$-A_2\left\{1+sR_3(C+C_2)-\frac{A_1[R_1+R_2(1+sR_1C_1)]}{R_1(1+A_1)+R_2(1+sR_1C_1)}\right\}$$

$$= \frac{R_4\{1+sR_3[C(1+A_2)+C_2]\}}{1-A_2+sR_3[C+C_2(1-A)]+\dfrac{A_1A_2[R_1+R_2(1+sR_1C_1)]}{R_1(1+A_1)+R_2(1+sR_1C_1)}\}}$$

$$= \frac{R_4\{1+sR_3[C(1+A_2)+C_2]\}[R_1(1+A_1)+R_2(1+sR_1C_1)]}{[R_1(1+A_1)+R_2(1+sR_1C_1)]\{1-A_2+sR_3[C+C_2(1-A_2)]\}}$$

$$+A_1A_2[R_1+R_2(1+sR_1C_1)]$$

$$= \frac{R_4\{1/A_2+sR_3[C(1+1/A_2)+C_2/A_2]\}[R_1+1/A_1)}{[R_1(1+1/A_1)+(R_2/A_1)(1+sR_1C_1)]\{1/A_2-1}$$

$$+(R_2/A_1)(1+sR_1C_1)]$$

$$+sR_3[C/A_2+C_2(1/A_2-1)]\}+R_1+R_2(1+sR_1C_1)$$

$$= R_4N(s)/D(s) \qquad (1\text{-}44)$$

Now the amplifier gains are given by

$$A_1 = A_{10}\,\omega_c/(s+\omega_c) \qquad (1\text{-}45)$$

and

$$A_2 = A_{20}\,\omega_c/(s+\omega_c)\ , \qquad (1\text{-}46)$$

therefore

$$1/A_1 = (1/A_{10})(1+s/\omega_c) = a_1(1+s/\omega_c) \qquad (1\text{-}47)$$

and

$$1/A_2 = (1/A_{20})(1+s/\omega_c) = a_2(1+s/\omega_c) \ . \qquad (1\text{-}48)$$

Since $a<<1$, second order terms in a will be neglected. Also assume that C_1, $C_2<<C$.

$$N(s) = \{R_1[1+a_1(1+s/\omega_c)]+a_1R_2(1+sR_1C_1)(1+s/\omega_c)\}[a_2(1+s/\omega_c)+sR_3\{C[1+a_2(1+s/\omega_c)]$$
$$+a_2C_2(1+s/\omega_c)\}]$$
$$\doteq a_2R_1(1+s/\omega_c)[1+a_1(1+s/\omega_c)]+sR_1R_3C[1+a_2(1+s/\omega_c)][1+a_1(1+s/\omega_c)]+a_2\,s\,R_1R_3C_2(1+s/\omega_c)$$
$$[1+a_1(1+s/\omega_c)]+a_1sR_2R_3C(1+sR_1C_1)(1+s/\omega_c)[1+a_2(1+s/\omega_c)]$$
$$\doteq a_2R_1(1+s/\omega_c)+sR_1R_3C[1+(a_1+a_2)(1+s/\omega_c)]+a_2sR_1R_3C_2(1+s/\omega_c)+a_1sR_2R_3C(1+sR_1C_1)(1+s/\omega_c)$$
$$= sR_1R_3\{C[1+(a_1+a_2)(1+s/\omega_c)]+a_2C_2(1+s/\omega_c)\}+a_1sR_2R_3C[1+s(R_1C_1+1/\omega_c)+s^2R_1C_1/\omega_c]$$
$$+a_2R_1(1+s/\omega_c)$$
$$= sR_1R_3[C(1+a_1+a_2)+a_2C_2]+(s^2R_1R_3/\omega_c)[C(a_1+a_2)+a_2C_2]+s[a_1R_2R_3C(1+s^2R_1C_1/\omega_c)+a_2R_1/\omega_c]$$
$$+a_1s^2R_2R_3C(R_1C_1+1/\omega_c)+a_2R_1$$
$$= s\{R_1R_3[C(1+a_1+a_2)+a_2C_2]+a_1R_2R_3C(1+s^2R_1C_1/\omega_c)+a_2R_1/\omega_c\}$$
$$+\ a_2R_1+s^2\{(R_1R_3/\omega_c)[C(a_1+a_2)+a_2C_2]+a_1R_2R_3C(R_1C_1+\ 1/\omega_c)\}$$
$$\doteq s[R_1R_3C(1+a_1+a_2)+a_1R_2R_3C+a_2R_1/\omega_c]+a_2R_1+(s^2/\omega_c)[R_1R_3C(a_1+a_2)+a_1R_2R_3C] \qquad (1\text{-}49)$$

$$D(s) = R_1+R_2(1+sR_1C_1)+\{R_1[1+a_1(1+s/\omega_c)]+a_1R_2(1+s/\omega_c)(1+sR_1C_1)\}$$
$$[a_2(1+s/\omega_c)-1+sR_3\{a_2C(1+s/\omega_c)+C_2[a_2(1+s/\omega_c)-1]\}]$$

$$\doteq R_1+R_2(1+sR_1C_1)+R_1[1+a_1(1+s/\omega_c)][a_2(1+s/\omega_c)-1]-a_1R_2(1+s/\omega_c)(1+sR_1C_1)$$
$$+a_2sR_1R_3(1+s/\omega_c)(C+C_2)-sR_1R_3C_2[1+a_1(1+s/\omega_c)]-a_1sR_2R_3C_2(1+sR_1C_1)(1+s/\omega_c)$$

$$\doteq -a_1R_2[1+s(R_1C_1+1/\omega_c)+s^2R_1C_1/\omega_c]+a_2sR_1R_3C(1+s/\omega_c)-sR_1R_3C_2(1+a_1s/\omega_c)$$
$$-a_1sR_2R_3C_2[1+s(R_1C_1+1/\omega_c)+s^2R_1C_1/\omega_c]+R_2+sR_1R_2C_1$$

$$\doteq R_2(1-a_1)+a_2s^2R_1R_3C/\omega_c+s[R_1(R_2C_1-R_3C_2)+a_2(R_1R_3C-R_2/\omega_c)] \qquad (1\text{-}50)$$

$$Z_{in}(j\omega) = R_4N(j\omega)/D(j\omega) =$$

$$\frac{R_4\{j\omega[R_1R_3C(1+a_1+a_2)+a_1R_2R_3C+a_2R_1/\omega_c]+a_2R_1-\omega^2[R_1R_3C(a_1+a_2)/\omega_c+a_1R_2R_3C/\omega_c]\}}{R_2(1-a_1)-a_2\omega^2R_1R_3C/\omega_c+j\omega[R_1(R_2C_1-R_3C_2)+a_2(R_1R_3C-R_2/\omega_c)]}$$

$$= \frac{A+jB}{C+jD} = \frac{(A+jB)(C-jD)}{C^2+D^2} = \frac{(AC+BD)+j(BC-AD)}{C^2+D^2} = R_{eq}+j\omega L_{eq} \qquad (1\text{-}51)$$

$$AC = R_4[R_2(1-a_1)-a_2\omega^2R_1R_3C/\omega_c]\{a_2R_1-\omega^2[R_1R_3C(a_1+a_2)/\omega_c+a_1R_2R_3C/\omega_c]\}$$

$$\doteq R_2R_4\{a_2R_1-\omega^2[R_1R_3C(a_1+a_2)/\omega_c+a_1R_2R_3C/\omega_c]\} \qquad (1\text{-}52)$$

$$BD = \omega^2 R_4[R_1R_3C(1+a_1+a_2)+a_1R_2R_3C+a_2R_1/\omega_c][R_1(R_2C_1-R_3C_2)+a_2(R_1R_3C-R_2/\omega_c)]$$

$$\doteq \omega^2 R_1R_4(R_2C_1-R_3C_2)[R_1R_3C(1+a_1+a_2)+a_1R_2R_3C+a_2R_1/\omega_c]+a_2\omega^2R_1R_3R_4C(R_1R_3C-R_2/\omega_c)$$

$$= \omega^2 R_1R_4\{(R_2C_1-R_3C_2)[R_1R_3C(1+a_1+a_2)+a_1R_2R_3C+a_2R_1/\omega_c]+a_2R_3C(R_1R_3C-R_2/\omega_c)\} \quad (1\text{-}53)$$

$$BC = \omega R_4[R_1R_3C(1+a_1+a_2)+a_1R_2R_3C+a_2R_1/\omega_c][R_2(1-a_1)-a_2\omega^2R_1R_3C/\omega_c]$$

$$\doteq \omega R_2R_4(1-a_1)[R_1R_3C(1+a_1+a_2)+a_1R_2R_3C+a_2R_1/\omega_c]-a_2\omega^3R_1^2R_3^2R_4C^2/\omega_c$$

$$\doteq \omega R_4[R_1R_2R_3C(1+a_2)+R_2(a_1R_2R_3C+a_2R_1/\omega_c)-a_2\omega^2R_1^2R_3^2C^2/\omega_c] \quad (1\text{-}54)$$

$$AD = \omega R_4[R_1(R_2C_1-R_3C_2)+a_2(R_1R_3C-R_2/\omega_c)]\{a_2R_1-\omega^2[R_1R_3C(a_1+a_2)/\omega_c+a_1R_2R_3C/\omega_c]\}$$

$$\doteq \omega R_1R_4(R_2C_1-R_3C_2)\{a_2R_1-\omega^2[R_1R_3C(a_1+a_2)/\omega_c+a_1R_2R_3C/\omega_c]\} \quad (1\text{-}55)$$

$$C^2 = [R_2(1-a_1)-a_2\omega^2R_1R_3C/\omega_c]^2 \doteq R_2^2(1-a_1)^2-2a_2(1-a_1)\omega^2R_1R_2R_3C/\omega_c$$

$$\doteq R_2^2(1-2a_1)-2a_2\omega^2R_1R_2R_3C/\omega_c \quad (1\text{-}56)$$

$$D^2 = [R_1(R_2C_1-R_3C_2)+a_2(R_1R_3C-R_2/\omega_c)]^2 << C^2 \quad (1\text{-}57)$$

$$AC+BD \doteq a_2R_1R_2R_4+\omega^2R_4\{R_1(R_2C_1-R_3C_2)[R_1R_3C(1+a_1+a_2)+a_1R_2R_3C+a_2R_1/\omega_c]+a_2R_1R_3C(R_1R_3C-R_2/\omega_c)$$
$$-R_2[R_1R_3C(a_1+a_2)/\omega_c+a_1R_2R_3C/\omega_c]\}$$
$$= a_2R_1R_2R_4+\omega^2R_4\{R_1(R_2C_1-R_3C_2)[R_1R_3C(1+a_1+a_2)+a_1R_2R_3C+a_2R_1/\omega_c]$$
$$+R_3C[a_2R_1(R_1R_3C-2R_2/\omega_c)-a_1R_2(R_1+R_2)/\omega_c]\} \quad (1\text{-}58)$$

$$BC-AD \doteq \omega R_4[R_1R_2R_3C(1+a_2)+R_2(a_1R_2R_3C+a_2R_1/\omega_c)-a_2\omega^2R_1^2R_3^2C^2/\omega_c-R_1(R_2C_1-R_3C_2)$$
$$\{a_2R_1-\omega^2[R_1R_3C(a_1+a_2)/(\omega_c+aR_2R_3C/\omega_c]\}]$$
$$\doteq \omega R_4[R_2R_3C(R_1+a_2R_1+a_1R_2)+(a_2R_1/\omega_c)(R_2-\omega^2R_1R_3^2C^2)] \quad (1\text{-}59)$$

$$L_{eq} = \frac{BC-AD}{C^2+D^2} \doteq \frac{BC-AD}{C^2} \quad (1\text{-}60)$$

$$L_{eq} \doteq (BC-AD)/\omega C^2 \doteq \frac{R_4[R_2R_3C(R_1+a_2R_1+a_1R_2)+a_2R_1(R_2-\omega^2R_1R_3^2C^2/\omega_c)]}{R_2^2(1-2a_1)-2a_2\omega^2R_1R_2R_3C/\omega_c}$$

$$= \frac{(R_4/R_2^2)[R_2R_3C(R_1+a_2R_1+a_1R_2)+a_2R_1(R_2-\omega^2R_1R_3^2C^2/\omega_c)]}{1-2(a_1+a_2\omega^2R_1R_3C/R_2\omega_c}$$

$$\doteq (R_4/R_2^2)[1+2(a_1+a_2\omega^2R_1R_3C/R_2\omega_c)][R_2R_3C(R_1+a_2R_1+a_1R_2)+a_2R_1(R_2-\omega^2R_1R_3^2C^2/\omega_c)]$$

$$\doteq (R_4/R_2^2)[R_2R_3C(R_1+a_2R_1+a_1R_2)+(a_2R_1/\omega_c)(R_2-\omega^2R_1R_3^2C^2)+2R_1R_2R_3C(a_1+a_2\omega^2R_1R_3C/R_2\omega_c)]$$

$$= (R_1R_3R_4C/R_2)[1+a_2+a_1R_2/R_1+(a_2/\omega_cR_2R_3C)(R_2-\omega^2R_1R_3^2C^2)+2a_1+2a_2\omega^2R_1R_3C/R_2\omega_c]$$

$$= (R_1R_3R_4C/R_2)[1+a_1(2+R_2/R_1)+a_2+(a_2\omega/\omega_c)(\omega R_1R_3C/R_2+1/\omega R_3C)] \qquad (1\text{-}61)$$

$$R_{eq} = \frac{AC+BD}{C^2+D^2} \doteq (AC+BD)/C^2$$

$$\doteq a_2R_1R_2R_4+\omega^2R_4\{R_1(R_2C_1-R_3C_2)[R_1R_3C(1+a_1+a_2)+a_1R_2R_3C+a_2R_1/\omega_c]+a_2R_1R_3C(R_1R_3C-R_2/\omega_c)$$
$$-R_2[R_1R_3C(a_1+a_2)/\omega_c+a_1R_2R_3C/\omega_c]\}$$
$$\frac{}{R_2^2(1-2a_1)-2a_2\omega^2R_1R_2R_3C/\omega_c}$$

$$= a_2R_1R_4/R_2+(\omega^2R_4/R_2^2)\{R_1(R_2C_1-R_3C_2)[R_1R_3C(1+a_1+a_2)+a_1R_2R_3C+a_2R_1/\omega_c]+a_2R_1R_3C(R_1R_3C-R_2/\omega_c)$$
$$-R_2[R_1R_3C(a_1+a_2)/\omega_c+a_1R_2R_3C/\omega_c]\}$$
$$\frac{}{1-2(a_1+a_2\omega^2R_1R_3C/R_2\omega_c)}$$

$$\doteq [1+2(a_1+a_2\omega^2R_1R_3C/R_2\omega_c)]\left[a_2R_1R_4/R_2+(\omega^2R_4/R_2^2)\{R_1(R_2C_1-R_3C_2)[R_1R_3C(1+a_1+a_2)\right.$$
$$\left.+a_1R_2R_3C+a_2R_1/\omega_c]+a_2R_1R_3C(R_1R_3C-R_2/\omega_c)-R_2[R_1R_3C(a_1+a_2)/\omega_c+a_1R_2R_3C/\omega_c]\}\right]$$

$$\doteq a_2R_1^2R_4/R_2+\omega^2R_1R_3R_4C(R_2C_1-R_3C_2)/R_2^2+(\omega^2R_4/R_2^2)\{a_2R_1^2R_3^2C^2-(R_1R_2R_3C/\omega_c)[2a_2+a_1(1+R_2/R_1)]\}$$

$$= (\omega R_1R_3R_4C/R_2)\{\omega R_1(R_2C_1-R_3C_2)/R_2+a_2(\omega R_1R_3C/R_2+1/\omega R_3C)-(\omega/\omega_c)[2a_2+a_1(1+R_2/R_1)]\}$$

(1-62)

$$D = \frac{1}{Q} = R_{eq}/L_{eq} \doteq \frac{\omega R_1(R_2C_1-R_3C_2)/R_2+a_2(\omega R_1R_3C/R_2+1/\omega R_3C)-(\omega/\omega_c)[2a_2+a_1(1+R_2/R_1)]}{1+a_1(2+R_2/R_1)+a_2+(a_2\omega/\omega_c\ (\omega R_1R_3C/R_2+1/\omega R_3C)}$$

$$= \omega R_1(R_2C_1-R_3C_2)/R_2+a_2(\omega R_1R_3C/R_2+1/\omega R_3C)-(\omega/\omega_c)[2a_2+a_1(1+R_2/R_1)] \qquad (1\text{-}63)$$

Now let $R_1 = R_2$ and $a_1 = a_2 = a$. The principal equations then become

$$L_{eq} = R_3R_4C[1 + 4a + (a\omega/\omega_c)(\omega R_3C + 1/\omega R_3C)] \qquad (1\text{-}64)$$

$$R_{eq} = \omega R_3R_4C[\omega(R_1C_1 - R_3C_2) + a(\omega R_3C + 1/\omega R_3C) - 4a\omega/\omega_c] \qquad (1\text{-}65)$$

$$D = \omega(R_1C_1 - R_3C_2) + a(\omega R_3C + 1/\omega R_3C) - 4a\omega/\omega_c. \qquad (1\text{-}66)$$

These expressions are in agreement with those found by Orchard and Sheahan [5] in a similar analysis of the Riordan gyrator. The equivalent inductor produced is almost identical to that found in the simplified analysis in the preceding section. However, a startling difference appears in the expression for the dissipation factor. Note that the last term in Eq. (1-66) is negative. Assume for the moment that the capacitances C_1 and C_2 are at their naturally occurring values of a few picofarads, and that $R_1 \doteq R_3$. Also assume that the product ωR_3C is somewhere near unity. If internally compensated operational amplifiers are used to construct the gyrator, then in general, $\omega >> \omega_c$, due to the fact that ω_c for these amplifiers is only a few Hertz. This means that the last term in Eq. (1-66) is dominant, and the net dissipation factor will be negative!

To correct for this possibly unstable condition, it may become necessary to augment C_1 with additional capacitance to force the dissipation factor to become positive. The significance of the foregoing analysis is that inductances

of almost unlimited value may be realized with extremely high Q-factors using the Riordan gyrator. The analysis also shows that the parameters of an inductor simulated using the Riordan gyrator do not depend, as is the case with several other gyrator circuits, upon exact cancellation of terms to form the proper impedance matrix, i.e., the Riordan gyrator does not suffer from sensitivity problems. An "inductorless" LC filter constructed using the Riordan gyrator to simulate the inductors would then have a sensitivity comparable to a normal LC filter. This characteristic of the Riordan is extremely significant with regard to active filter design.

E. REALIZATION OF AN UNGROUNDED INDUCTOR

Up to this point in the analysis, only the realization of an inductor with one terminal grounded has been discussed. Obviously, a circuit designer would be hard pressed to work only with grounded inductors, therefore the problem of realizing an ungrounded or "floating" inductor must be analyzed.

One method of obtaining a floating inductor is to place a capacitor in shunt between two gyrators as shown in Fig. 1.4. Assuming the gyrators to be lossless, the chain matrix for the two-port formed by the two gyrators and the capacitor is given by

$$\begin{bmatrix} A & B \\ C & D \end{bmatrix} = \begin{bmatrix} 0 & -R_3 \\ -1/R_4 & 0 \end{bmatrix} \begin{bmatrix} 1 & 0 \\ sC & 1 \end{bmatrix} \begin{bmatrix} 0 & -R'_3 \\ -1/R'_4 & 0 \end{bmatrix} = \begin{bmatrix} -sR_3C & -R_3 \\ -1/R_4 & 0 \end{bmatrix} \begin{bmatrix} 0 & -R'_3 \\ -1/R'_4 & 0 \end{bmatrix} =$$

$$\begin{bmatrix} R_3/R'_4 & sR_3R'_3 \\ 0 & R'_3/R_4 \end{bmatrix} . \quad (1\text{-}67)$$

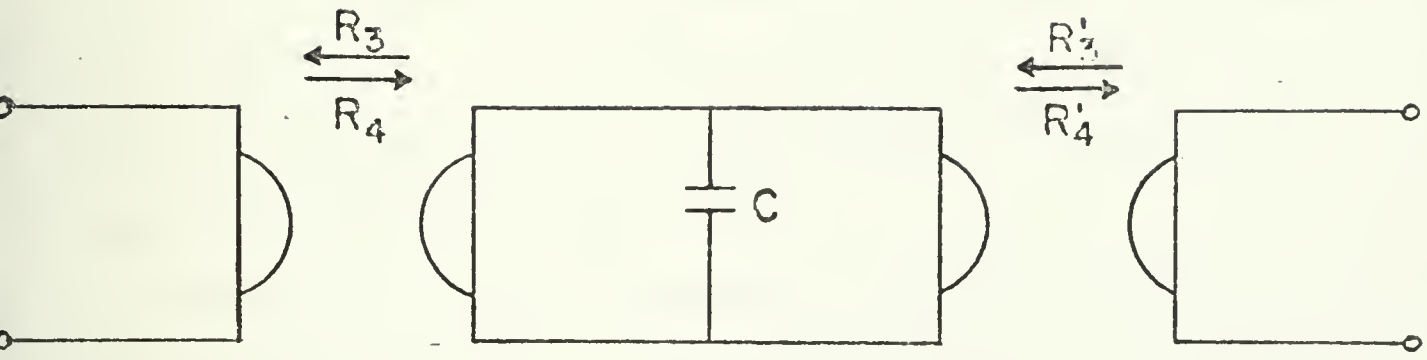

Figure 1.4. Circuit to Produce a Floating Inductor

The admittance matrix for the circuit is then

$$\begin{bmatrix} y_{11} & y_{12} \\ y_{21} & y_{22} \end{bmatrix} = \begin{bmatrix} D/B & C-AD/B \\ -1/B & A/B \end{bmatrix} = \begin{bmatrix} 1/sR_3R_4C & -1/sR_4R'_4C \\ -1/sR_3R'_3C & 1/sR'_3R'_4C \end{bmatrix} . \tag{1-68}$$

The admittance matrix for a single floating inductor is

$$\begin{bmatrix} y_{11} & y_{12} \\ y_{21} & y_{22} \end{bmatrix} = \begin{bmatrix} 1/sL & -1/sL \\ -1/sL & 1/sL \end{bmatrix} . \tag{1-69}$$

To equate this result to that obtained by combining two gyrators and a capacitor, the following conditions must hold:

$$R_3R_4 = R_4R'_4 = R_3R'_3 = R'_3R'_3 . \tag{1-70}$$

Therefore the conditions

$$R_3 = R'_4 . \tag{1-71}$$

and

$$R_3' = R_4 \tag{1-72}$$

must be satisfied to present a single floating inductor. Otherwise, parasitic inductances to ground will be present. This high degree of sensitivity to component tolerance is entirely unsatisfactory, so other means of producing a floating inductor must be sought.

Riordan [3] himself suggested a circuit based upon his original gyrator circuit which would realize a floating inductor. However, he admitted that this circuit too suffered from sensitivity problems which could result in a parasitic inductance to ground.

Several other gyrator circuits have been proposed in an attempt to solve the floating inductor problem, but they all seem to suffer from low Q, parasitics to ground, or other problems due to the requirement for exact component selection. Perhaps, then, an advisable approach to the problem of realizing a floating inductor might be to realize it as part of some total configuration rather than as a single element.

F. REALIZATION OF AN INDUCTIVE PI NETWORK

Orchard and Sheahan [5] discussed a circuit based upon an idea by Gorski-Popiel [6] which transforms a pi of resistance into a pi of inductances. The circuit consists of two Riordan gyrators placed back-to-back with an additional series resistance between them as shown in Fig. 1.5.

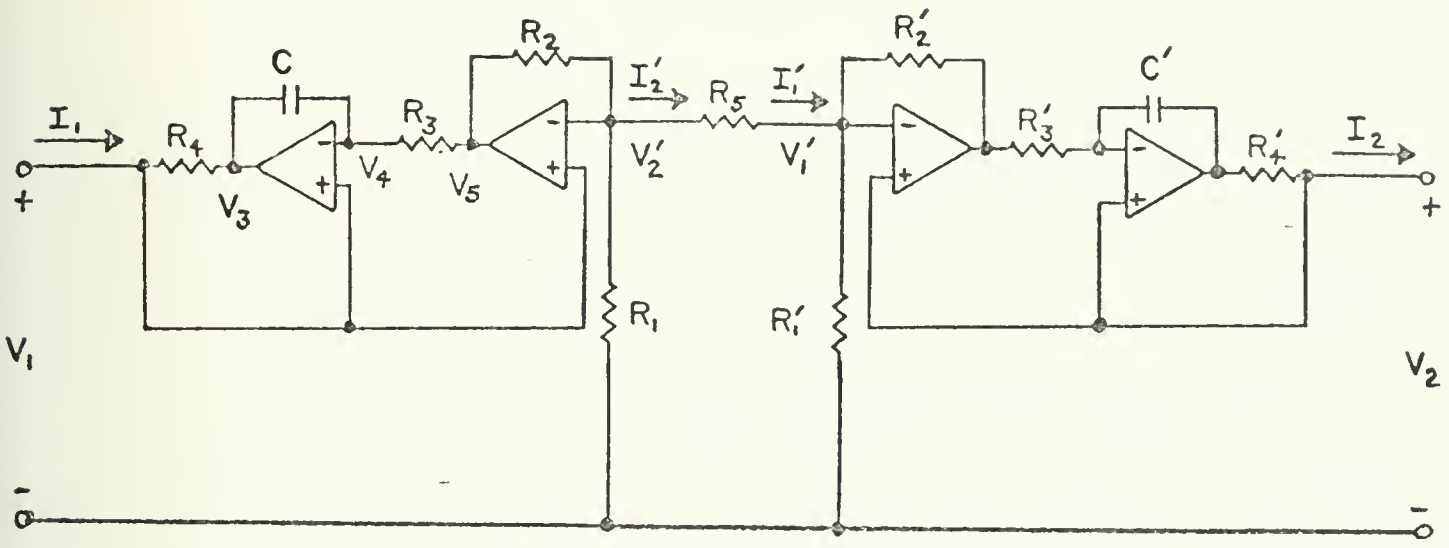

Figure 1.5. The "Dual" Riordan Gyrator

To simplify the analysis of the circuit, ideal amplifiers are assumed, i.e., having infinite gains, infinite input impedances, and zero output impedances. Also, the Q-adjusting capacitors are omitted; however, the effect of these would be as before. To work on the entire circuit simultaneously would result in rather cumbersome equations, therefore it is advantageous to solve the circuit piecemeal, namely by dividing it into three parts consisting of the left-hand gyrator, the series resistor R_5, and the right-hand gyrator. The chain matrices for each of these three sections may be found easily, then the chain matrix for the entire circuit may be obtained by multiplying the three chain matrices together.

First, consider the left-hand gyrator. When $I_2' = 0$:

$$V_5 = V_1(1+R_2/R_1) \qquad (1\text{-}73)$$

$$V_3 = V_1[1+(1/sC)/R_3] - V_5(1/sC)/R_3$$

$$= V_1(1+1/sR_3C) - V_1(1/sR_3C)(1+R_2/R_1)$$

$$= V_1(1-R_2/sR_1R_3C) \qquad (1\text{-}74)$$

$$I_1 = (V_1-V_3)/R_4 = (V_1/R_4)[1-(1-R_2/sR_1R_3C)]$$

$$= V_1(R_2/sR_1R_3R_4C) \qquad (1\text{-}75)$$

$$V_2' = V_5[R_1/(R_1+R_2)] = V_1[R_1/(R_1+R_2)](1+R_2/R_1) = V_1 \qquad (1\text{-}76)$$

$$A_1 = \frac{V_1}{V_2'}\Big|_{I_2'=0} = 1 \qquad (1\text{-}77)$$

$$C_1 = \frac{I_1}{V_2'}\Big|_{I_2'=0} = R_2/sR_1R_3R_4C \ . \qquad (1\text{-}78)$$

Now when $V_2' = 0$:

$$V_5 = AV_1 \qquad (1\text{-}79)$$

$$V_3 = V_1(1+1/sR_3C) - V_5(1/sR_3C)$$

$$= V_1(1+1/sR_3C) - AV_1(1/sR_3C) = -AV_1/sR_3C \qquad (1\text{-}80)$$

$$I_2' = V_5/R_2 = AV_1/R_2 \qquad (1\text{-}81)$$

$$I_1 = (V_1-V_3)/R_4 = (V_1/R_4)(1+A/sR_3C) = AV_1/sR_3R_4C \qquad (1\text{-}82)$$

$$B_1 = \frac{V_1}{I_2'}\Big|_{V_2'=0} = R_2/A = 0 \qquad (1\text{-}83)$$

$$D_1 = \frac{I_1}{I_2'}\Big|_{V_2'=0} = R_2/sR_3R_4C \ . \qquad (1\text{-}84)$$

Now consider the resistor R_5.

$$A_2 = \frac{V_2'}{V_1'}\Big|_{I_1'=0} = 1 \tag{1-85}$$

$$B_2 = \frac{V_2'}{I_1'}\Big|_{V_1'=0} = R_5 \tag{1-86}$$

$$C_2 = \frac{I_2'}{V_1'}\Big|_{I_1'=0} = 0 \tag{1-87}$$

$$D_2 = \frac{I_2'}{I_1'}\Big|_{V_1'=0} = 1 \tag{1-88}$$

Finally consider the right-hand gyrator. Except for notational differences, it is the same as the left-hand gyrator turned around. Its chain matrix, therefore, is the inverse of the chain matrix of the left-hand gyrator, except that primed variables are substituted for the unprimed variables as follows:

$$\begin{bmatrix} A_3 & B_3 \\ C_3 & D_3 \end{bmatrix} = \begin{bmatrix} A_1' & B_1' \\ C_1' & D_1' \end{bmatrix}^{-1} = \frac{1}{A_1'D_1' - B_1'C_1'} \begin{bmatrix} D_1' & -B_1' \\ -C_1' & A_1' \end{bmatrix}$$

$$= (sR_3'R_4'C'/R_2') \begin{bmatrix} R_2'/sR_3'R_4'C' & 0 \\ R_2'/sR_1'R_3'R_4'C' & 1 \end{bmatrix}$$

$$= \begin{bmatrix} 1 & 0 \\ 1/R_1' & sR_3'R_4'C'/R_2' \end{bmatrix} . \tag{1-89}$$

Therefore, the chain matrix for the entire circuit is given by

$$\begin{bmatrix} A & B \\ C & D \end{bmatrix} = \begin{bmatrix} 1 & 0 \\ R_2/sR_1R_3R_4C & R_2/sR_3R_4C \end{bmatrix} \begin{bmatrix} 1 & R_5 \\ 0 & 1 \end{bmatrix} \begin{bmatrix} 1 & 0 \\ 1/R_1' & sR_3'R_4'C'/R_2' \end{bmatrix}$$

$$= \begin{bmatrix} 1 & R_5 \\ R_2/sR_1R_3R_4C & (R_2/sR_3R_4C)(1+R_5/R_1) \end{bmatrix} \begin{bmatrix} 1 & 0 \\ 1/R_1' & sR_3'R_4'C'/R_2' \end{bmatrix}$$

$$= \begin{bmatrix} 1+R_5/R_1' & sR_3'R_4'R_5C'/R_2' \\ (R_2/sR_1R_3R_4C)[1+(R_1+R_5)/R_1'] & R_2R_3'R_4'C'(R_1+R_5)/R_1R_2'R_3R_4C \end{bmatrix}$$

(1-90)

It will be shown that the effect of an imbalance between the two gyrators, namely a difference between the quantities $R_3'R_4'C'/R_2'$ and R_3R_4C/R_2 will result in the introduction of an ideal transformer of near unity voltage ratio in cascade with the resulting inductive pi network. Consider the circuit in Fig. 1.6. The chain matrix for the entire circuit is obtained by multiplying the chain matrix for the inductive pi network with that of the ideal transformer.

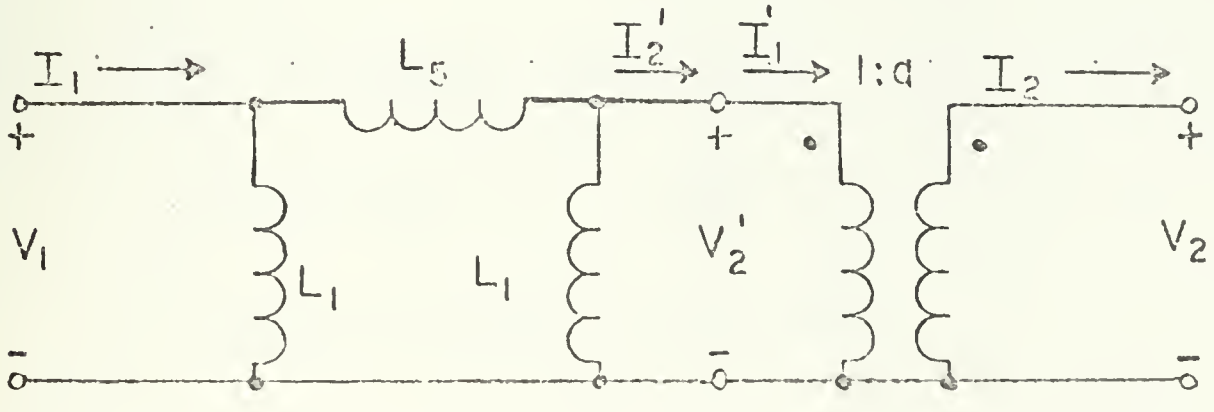

Figure 1.6. Inductive Pi in Cascade with Ideal Transformer

For the inductive pi network:

$$A_1 = \frac{V_1}{V_2'}\Big|_{I_2'=0} = 1/[L_1'/(L_1+L_5)] = 1 + L_5/L_1' \qquad (1\text{-}91)$$

$$B_1 = \frac{V_1}{I_2'}\Big|_{V_2'=0} = sL_5 \qquad (1\text{-}92)$$

$$C_1 = \frac{I_1}{V_2'}\Big|_{I_2'=0} = 1/sL_1'[L_1/(L_1+L_5+L_1')] = (L_1+L_5+L_1')/sL_1'L_1 \qquad (1\text{-}93)$$

$$D_1 = \frac{I_1}{I_2'}\Big|_{V_2'=0} = 1/[L_1/(L_1+L_5)] = 1+L_5/L_1 \ . \qquad (1\text{-}94)$$

For the ideal transformer:

$$A_2 = \frac{V_2'}{V_2}\Big|_{I_2=0} = 1/a \qquad (1\text{-}95)$$

$$B_2 = \frac{V_2'}{I_2}\Big|_{V_2=0} = 0 \qquad (1\text{-}96)$$

$$C_2 = \frac{I_1'}{V_2}\Big|_{I_2=0} = 0 \qquad (1\text{-}97)$$

$$D_2 = \frac{I_1'}{I_2}\Big|_{V_2=0} = a \ . \qquad (1\text{-}98)$$

Therefore for the entire circuit:

$$\begin{bmatrix} A & B \\ C & D \end{bmatrix} = \begin{bmatrix} 1+L_5/L_1' & sL_5 \\ (L_1+L_5+L_1')/sL_1'L_1 & 1+L_5/L_1 \end{bmatrix} \begin{bmatrix} 1/a & 0 \\ 0 & a \end{bmatrix}$$

$$= \begin{bmatrix} (1+L_5/L_1')/a & sL_5/a \\ (L_1+L_5+L_1'/asL_1'L_1 & a(1+L_5/L_1) \end{bmatrix} \ . \qquad (1\text{-}99)$$

Equating the elements of this chain matrix to those of the "dual-Riordan" circuit's chain matrix yields

$$(1+L_5/L_1')/a = 1+R_5/R_1' \tag{1-100}$$

$$L_5/a = R_3'R_4'R_5C'/R_2' \tag{1-101}$$

$$(L_1+L_5+L_1')/aL_1'L_1 = R_2[1+(R_1+R_5)/R_1']/R_1R_3R_4C \tag{1-102}$$

$$a(1+L_5/L_1) = R_2R_3'R_4'C'(R_1+R_5)/R_1R_2'R_3R_4C\ . \tag{1-103}$$

Solution of Eqs. (1-100) through (1-103) for L_1, L_1', L_5, and a yields

$$a = (R_2'R_3R_4C/R_2R_3'R_4'C')^{1/2} \tag{1-104}$$

$$L_1 = R_1R_3R_4C/R_2[1+R_1(1-a)/R_5] \tag{1-105}$$

$$L_1' = R_1'R_3R_4C/R_2[a+R_1'(a-1)/R_5] \tag{1-106}$$

$$L_5 = R_3R_4R_5C/R_2\ . \tag{1-107}$$

Now if a is reasonably close to unity, to a good approximation, the following equations are valid:

$$a \doteq 1 \tag{1-108}$$

$$L_1 \doteq AR_1[1-R_1(1-a)/R_5] \tag{1-109}$$

$$L_1' \doteq AR_1'[1-R_1'(a-1)/aR_5]/a \tag{1-110}$$

$$L_5 = AR_5 \tag{1-111}$$

where $A = R_3R_4C/R_2$.

For the ideal case where $R_3R_4C/R_2 = R_3'R_4'C'/R_2'$, i.e., a = 1, the transformation in Fig. 1.7 results.

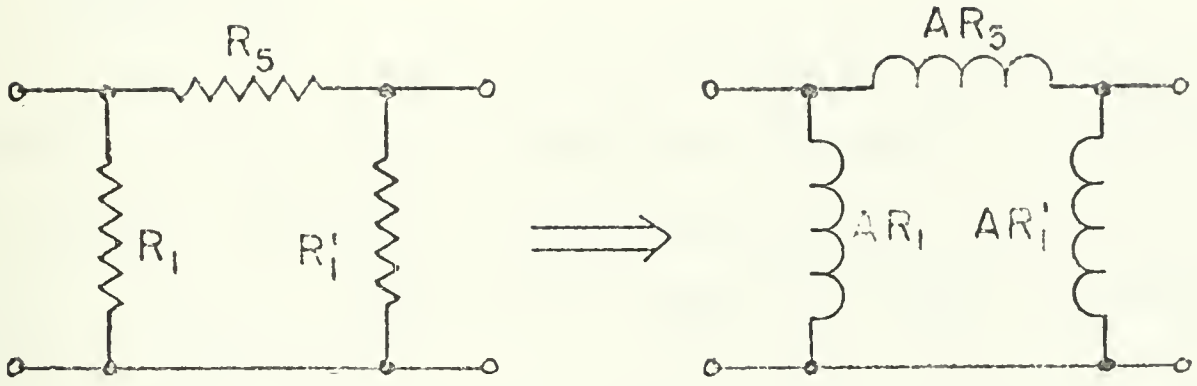

Figure 1.7. Formation of Inductive Pi

For precision (1% tolerance) components, the above representation of the gyrator-produced inductive pi network is sufficiently close to reality to use as a building block in electrical filter design. In the following chapter, it will be shown how this building block is best utilized in electrical filters.

II. IMPEDANCE TRANSFORMATION

A. INTRODUCTION

In 1928, E. L. Norton [7] introduced an impedance transforming technique which enables simultaneous transformation of impedance level and desired filtering in an electrical filter circuit. Reference [8] contains a good discussion of Norton's technique.

Basically, Norton's transformer filter sections are the equivalent of a normal filter section in cascade with an ideal transformer. Thus the attenuation and phase characteristics of the original filter section are retained, while the ideal transformer changes the impedance level.

The basis for Norton's technique is the pair of equivalences shown in Figs. 2.1 and 2.2.

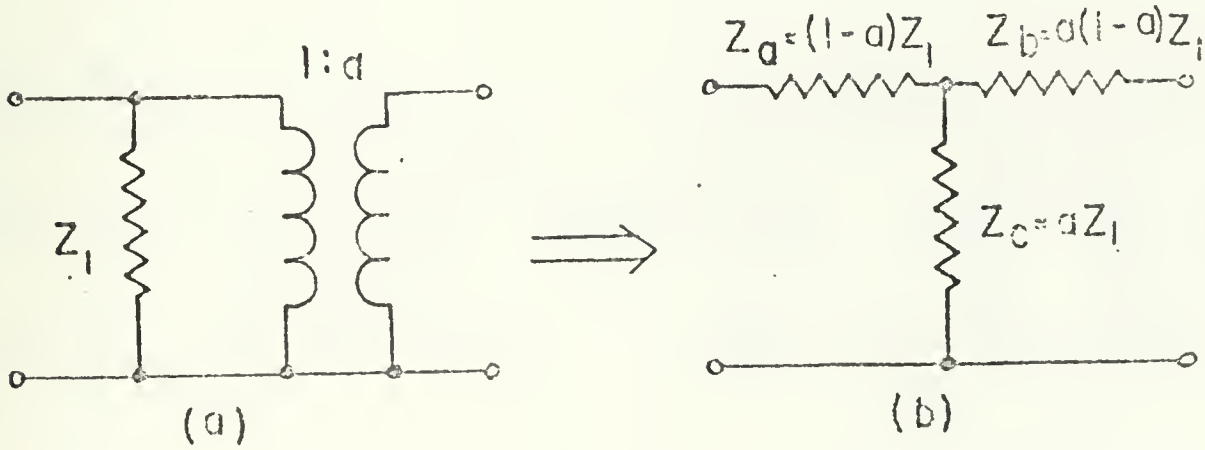

Figure 2.1. Tee Equivalent Circuit

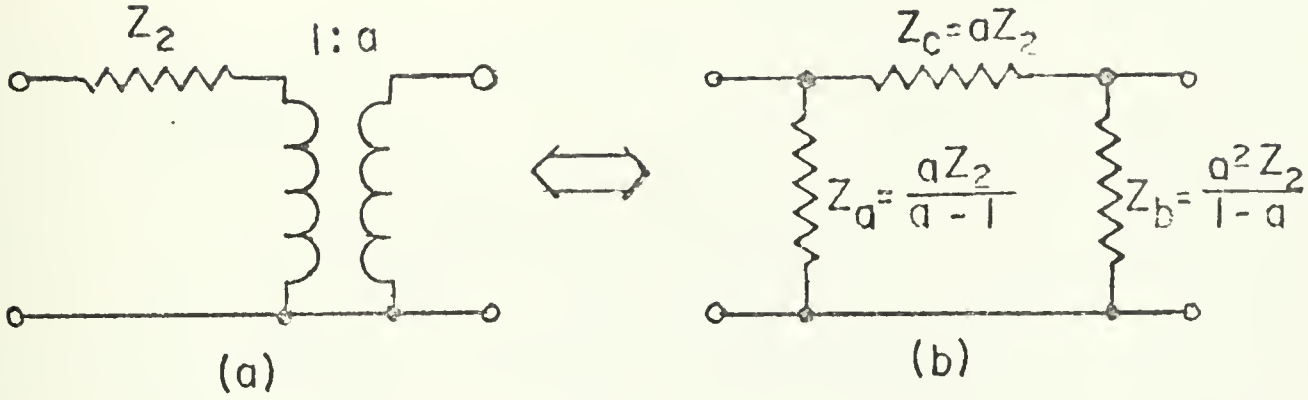

Figure 2.2. Pi Equivalent Circuit

Consider only the pair of circuits in Fig. 2.2 for a moment. Since the two circuits are equivalent, the addition of equal loads across the output port of each circuit will not affect the equivalence, as shown in Fig. 2.3.

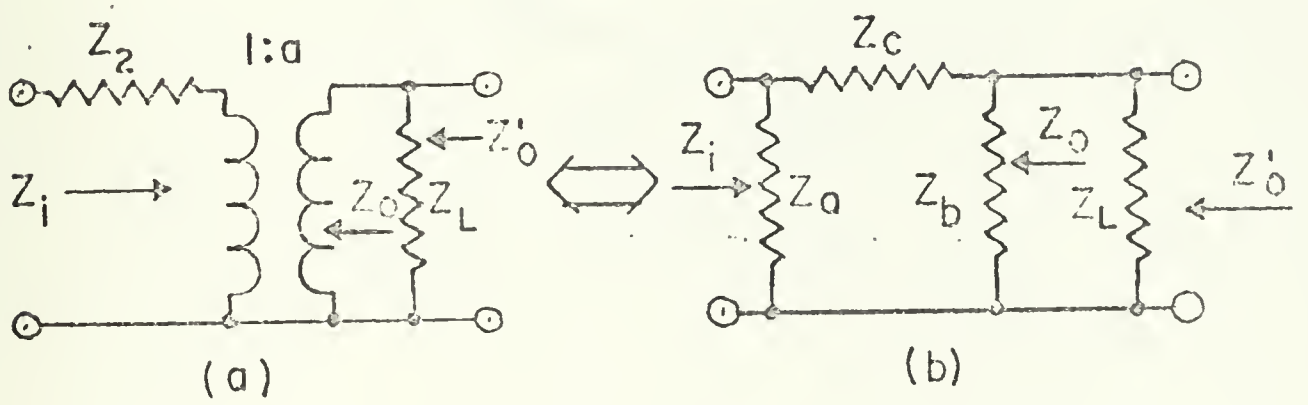

Figure 2.3. Loaded Pi Equivalent Circuit.

The transformer in Fig. 2.3(a) may be moved to the right of Z_L, changing the value of Z_L but leaving Z_i and Z'_o undisturbed, as shown in Fig. 2.4.

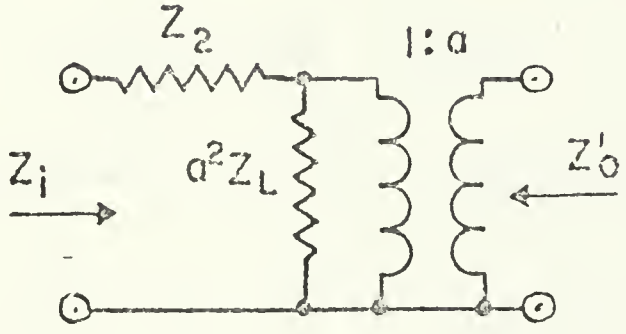

Figure 2.4. Effect of Shifting Transformer

If the transformer is removed completely, the circuit is as shown in Fig. 2.5.

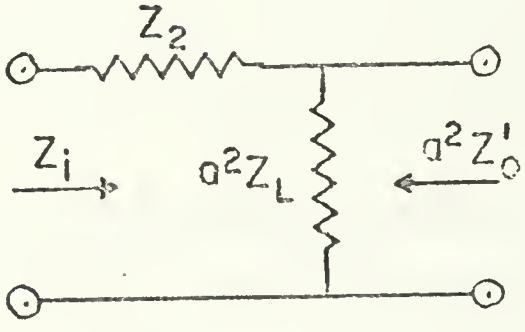

Figure 2.5. Effect of Removing Transformer

The sequence of circuits in Fig. 2.6 indicates how the Norton procedure may be used to modify the form of a circuit.

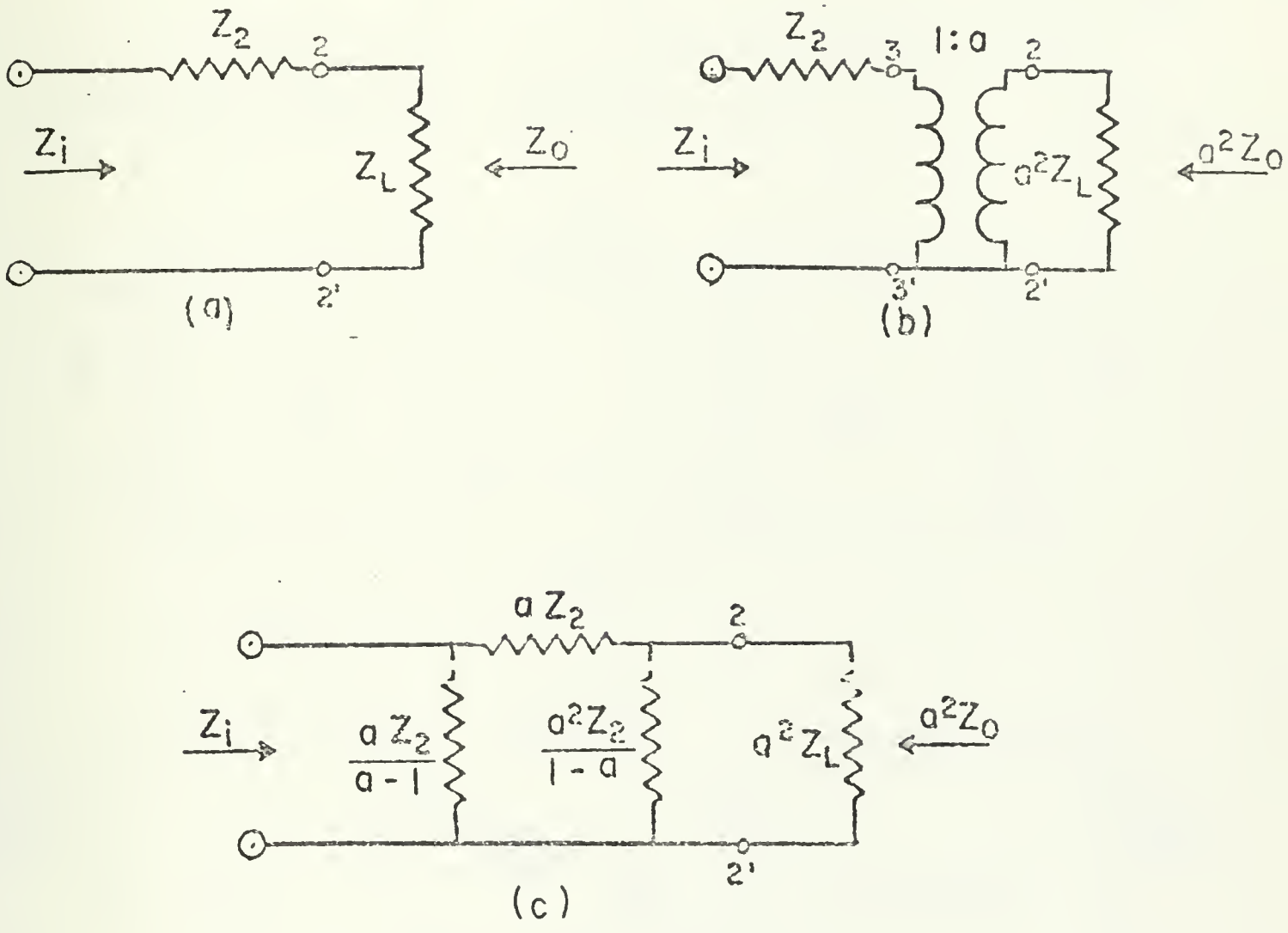

Figure 2.6. Series To Pi Transformation.

B. APPLICATION TO INDUCTORLESS FILTERS

As previously stated, there presently exists no entirely satisfactory way to simulate a single floating inductor. The Riordan gyrator may be used to simulate either a grounded inductor or a pi network of inductors. Therefore when synthesizing an inductorless filter using the Riordan circuits,

it is necessary to ensure that all of the inductors in the filter to be constructed appear either as single grounded inductors or in the pi configuration.

If a series inductor appears in the original filter circuit to be constructed, it must then be replaced by the inductive pi network as indicated in Fig. 2.7.

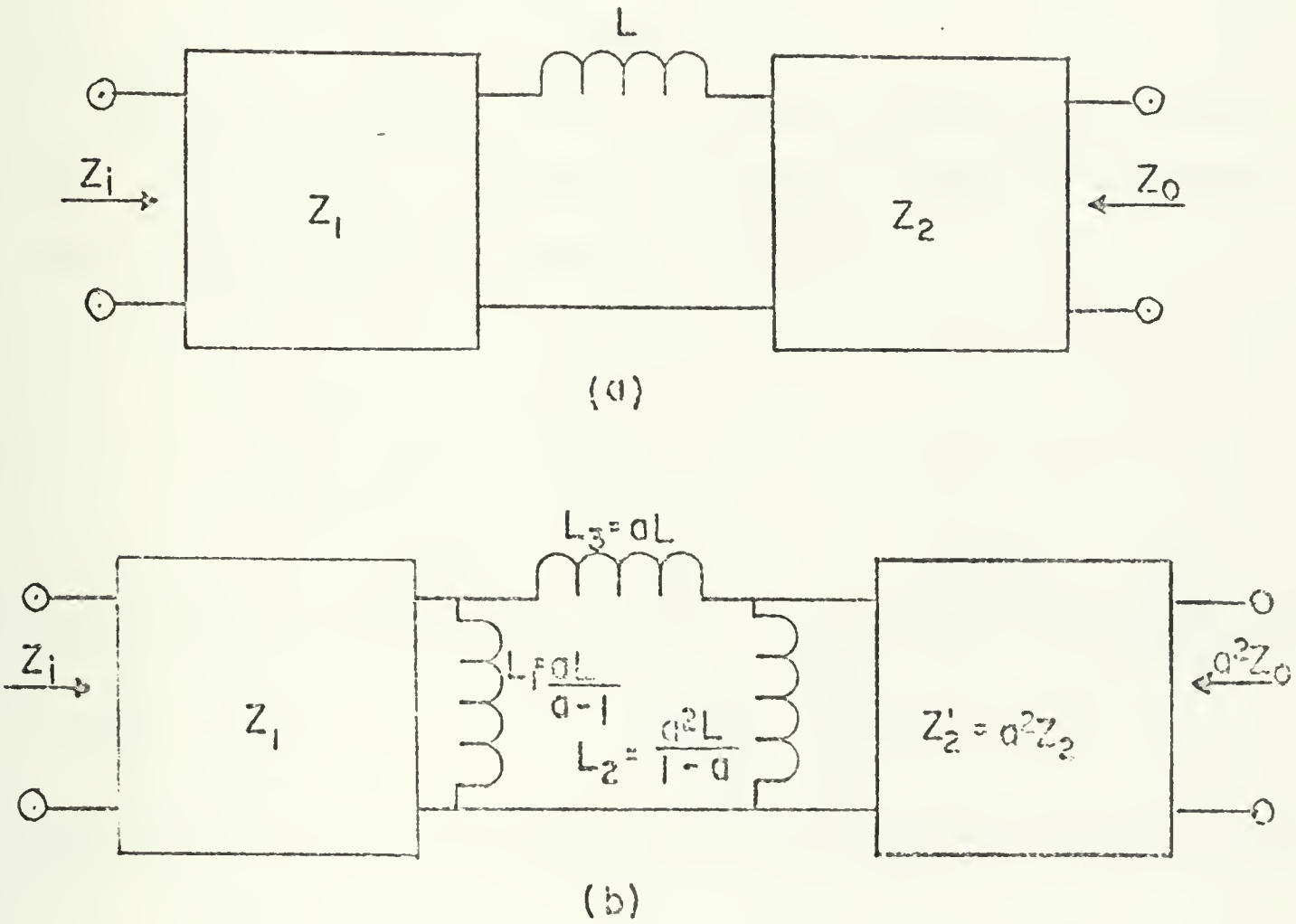

Figure 2.7. Replacement of Series Inductor.

Note that one of the shunt inductors in the pi network will be negative. This means that to obtain a physically realizable circuit, the negative inductor must combine with a positive inductor from the rest of the circuit to produce a

net value which is positive. Thus if $a > 1$, L_2 will be negative, and the first element in Z_2' must be a shunt inductor whose value is less than the magnitude of L_2; conversely, if $a < 1$, L_1 will be negative, and the last element in Z_1 must be a shunt inductor whose value is less than the magnitude of L_1.

C. BANDPASS FILTER TRANSFORMATION

The basic bandpass filter structure is as shown in Fig. 2.8, and consists of parallel-resonant LC circuits to ground, connected by series-resonant LC circuits.

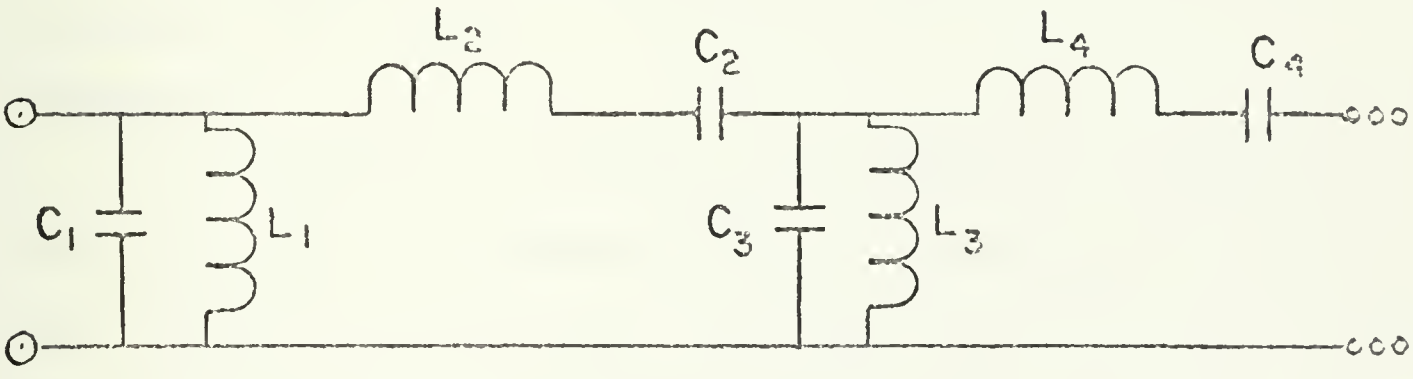

Figure 2.8. Basic Bandpass Filter Structure.

To realize this circuit as an inductorless filter using the Riordan gyrator, it is necessary to replace all series inductors L_2, L_4, ..., L_{2n} by their pi equivalent circuits.

Recall that when operating on a series inductance in a network, the input impedance remains constant, while the output impedance is changed. Therefore, for a filter circuit with equal terminations, in order to maintain the same transfer characteristics, it is necessary to bisect the filter circuit at the point of symmetry, then perform identical operations on each half in symmetrical fashion, i.e., by starting at the input and output ports of the filter and working toward the bisection point. As a result of this procedure, the new impedances looking into the two halves back toward the source and load, respectively, may have changed from their original values, but will still be equal, thus preserving the original filter characteristics.

To illustrate this procedure, consider the following example.

Example 1.

It is desired to construct the bandpass filter shown in Fig. 2.9 using the Riordan gyrator to simulate all inductors. For component standardization purposes, it is desired to make as many inductors and capacitors as possible have the same value. The circuit must first be made symmetrical so that it can be bisected. This is done by splitting C_3 and L_3 into equal parts. After bisection, the half-circuit shown in Fig. 2.10 results. Now the series inductor L_2 is transformed into a pi network, with the negative shunt inductor placed in parallel with L_1 as shown in Fig. 2.11.

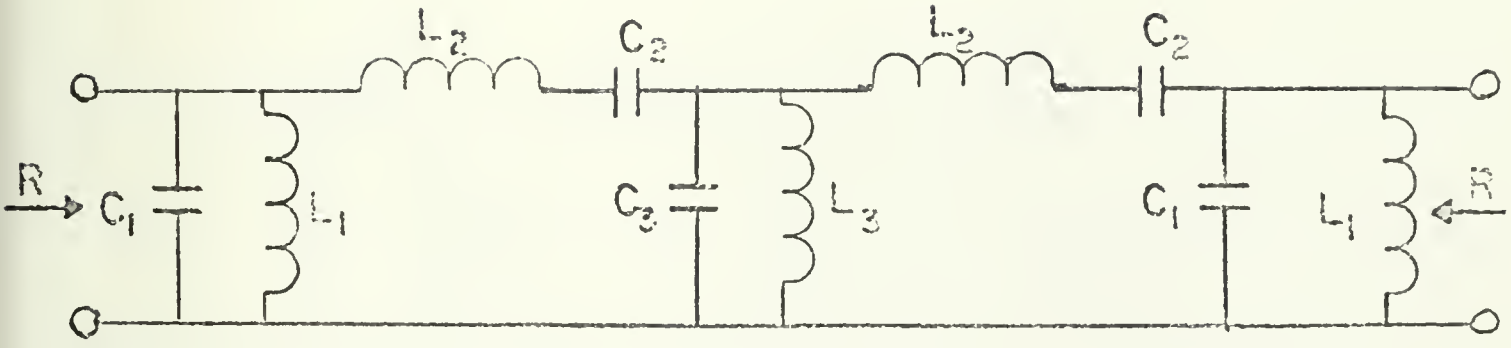

Figure 2.9. Conventional Bandpass Filter.

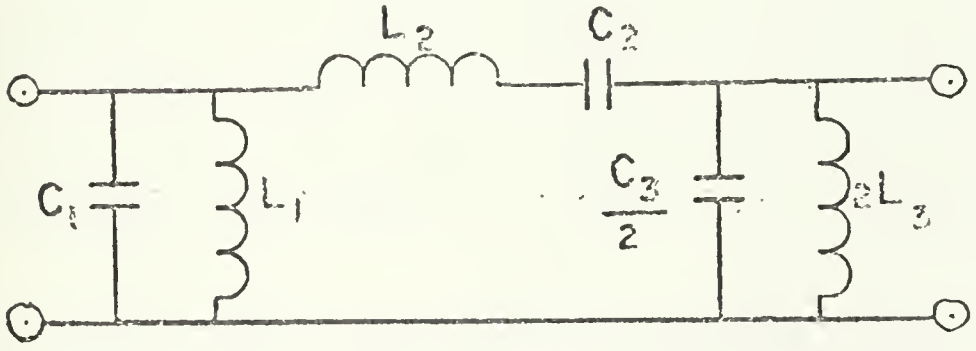

Figure 10. Half of Bisected Filter.

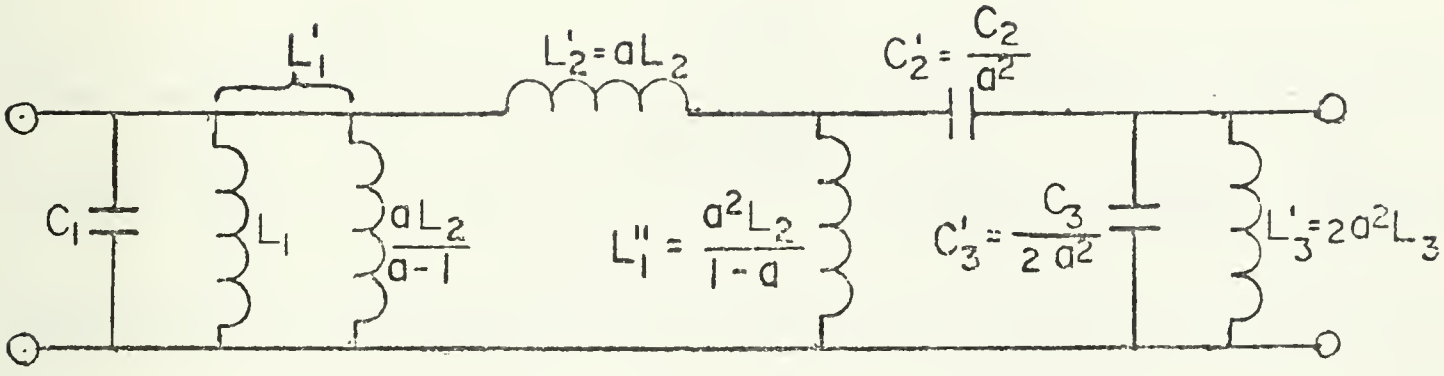

Figure 2.11. Half-Circuit After First Transformation.

Solving for a so that the new inductances L_1' and L_1'' are equal:

$$L_1[aL_2/(a-1)]/[L_1 + aL_2/(a-1)] = a^2L_2/(1-a) \qquad (2\text{-}1)$$

$$aL_1L_2/[L_1(a-1) + aL_2] = a^2L_2/(1-a) \qquad (2\text{-}2)$$

$$a[a(L_1 + L_2) - L_1] = (1-a)L_1 \qquad (2\text{-}3)$$

$$a = [L_1/(L_1 + L_2)]^{1/2}. \qquad (2\text{-}4)$$

Now the series capacitance C_2' is transformed into a capacitive pi network, with the negative shunt capacitor placed in parallel with C_3' as shown in Fig. 2.12.

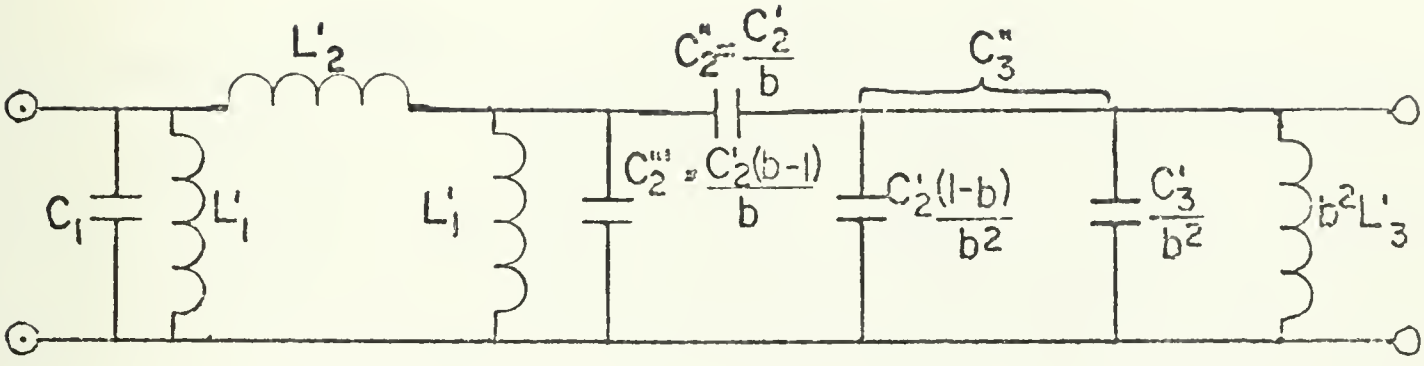

Figure 2.12. Half-Circuit After Second Transformation.

Solving for b so that the new capacitances C_2''' and C_3'' will have a ratio of two to one:

$$C_2'(b-1)/b = 2[C_2'(1-b)/b^2 + C_3'/b^2] \qquad (2\text{-}5)$$

$$C_2'[b(b-1) - 2(1-b)] = 2C_3' \qquad (2\text{-}6)$$

$$b^2 + b - (2 + C_3'/C_2') = 0 \qquad (2\text{-}7)$$

$$b = (1/2)[1+4(2+C_3'/C_2')]^{1/2} - 1/2$$

$$= 1/2[9 + 2C_3/C_2]^{1/2} - 1/2 \; . \qquad (2\text{-}8)$$

Thus the final transformed half-circuit is as shown in Fig. 2.13.

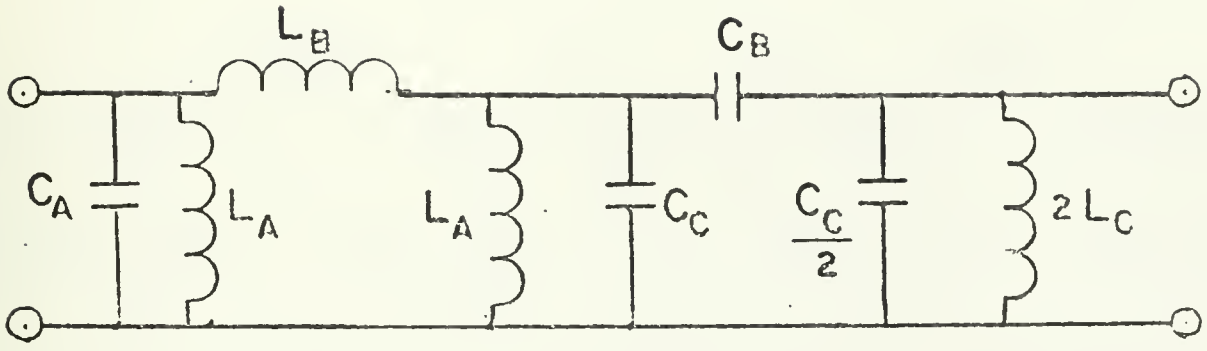

Figure. 2.13. Fully Transformed Half-Circuit.

The element values for the circuit of Fig. 2.13 are given by

$$C_A = C_1 \tag{2-9}$$

$$L_A = a^2L_2/(1-a) = L_1L_2/\{L_1+L_2 - [L_1(L_1+L_2)]^{1/2}\} \tag{2-10}$$

$$L_B = aL_2 = L_2[L_1/(L_1+L_2)]^{1/2} \tag{2-11}$$

$$C_B = C_2/a^2b = 2C_2(1+L_2/L_1)/[(9+2C_3/C_2)^{1/2}-1] \tag{2-12}$$

$$C_C = (b-1)C_2/a^2b$$

$$= C_2(1+L_2/L_1)[(9+2C_3/C_2)^{1/2}-3]/[(9+2C_3/C_2)^{1/2}-1] \tag{2-13}$$

$$L_C = a^2b^2L_3 = [L_1L_3/4(L_1+L_2)][(9+2C_3/C_2)^{1/2}-1]^2 \ . \tag{2-14}$$

After recombining the two half-circuits, the transformed bandpass filter thus produced is as shown in Fig. 2.14.

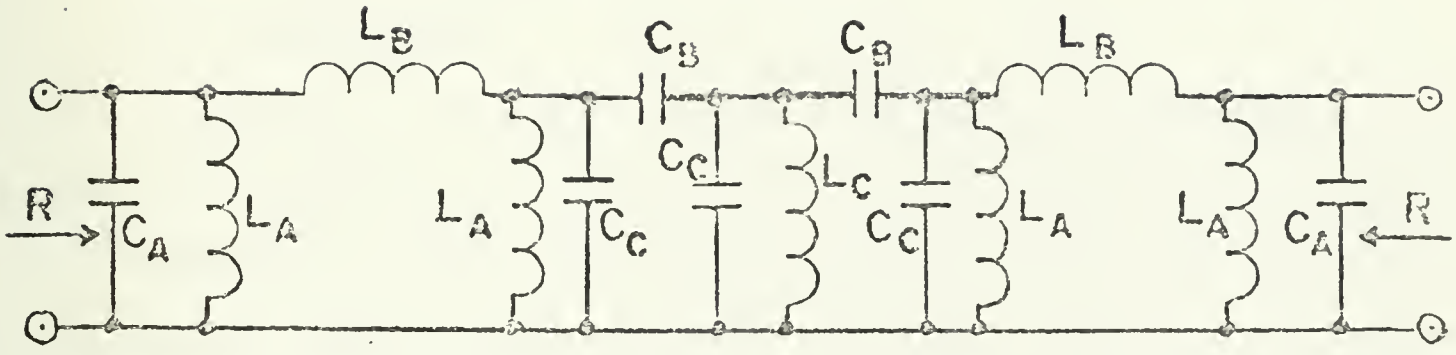

Figure 2.14. Transformed Bandpass Filter.

The transformed circuit contains two inductive pi networks and a single grounded inductor, and therefore requires two "dual" Riordan gyrators and one "single" Riordan gyrator.

D. SUMMARY

It is worthwhile to note that in the process of impedance transformation, the total number of elements in a filter circuit may increase significantly. However, this is the price which must be paid in order to arrive at a circuit suitable for simulation of the inductances. In low-frequency circuits, though, the savings in the size of a filter due to elimination of large bulky inductors should more than compensate for the addition of a few capacitors.

III. CONSTRUCTION OF AN INDUCTORLESS BANDPASS FILTER

A. IMAGE-PARAMETER FILTER STRUCTURES

1. Introduction

Chapter II indicated how a conventional bandpass filter structure, as might be used to construct a Butterworth or Tchebycheff filter, may be altered to a form suitable for simulation using Riordan gyrator circuits. Some filter structures do exist, however, which lend themselves to direct application of the Riordan circuits.

The ITT Handbook [9] contains a good deal of information concerning image-parameter filters. Because image-parameter filters are based in general upon physically unrealizable terminations, this classic filter type has to a large extent fallen by the wayside in recent years. Nevertheless, certain of the image-parameter filters do work quite well, and of these, several types of filter sections lend themselves very easily to construction using the Riordan gyrator circuits. Two of the bandpass filter sections in Ref. [9] were chosen for investigation and subsequent use in constructing an inductorless bandpass filter.

2. The Three-Element Shunt I Bandpass Filter Section

The three-element shunt I bandpass filter section is shown in Fig. 3.1.

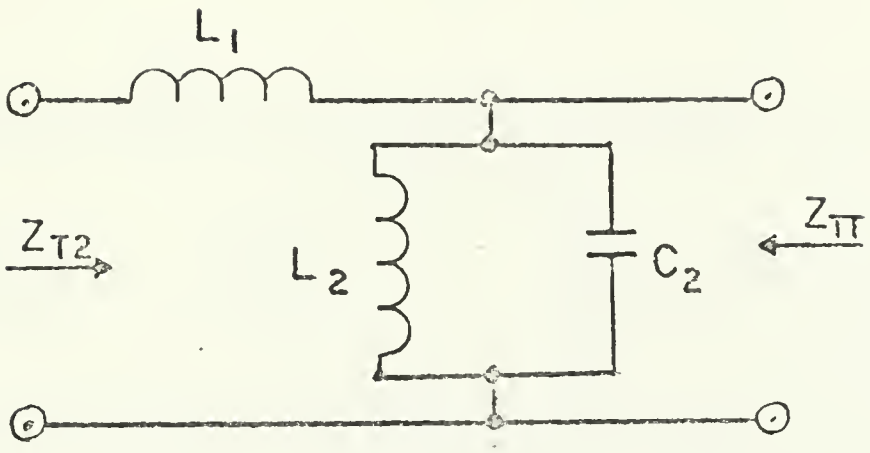

Figure 3.1. 3-Element Shunt I Bandpass Filter Section

Element values for the filter section are given by:

$$L_1 = (1+m)R/(1+m)(\omega_2-\omega_1) = R/2\pi(f_1+f_2) \qquad (3\text{-}1)$$

$$L_2 = R(\omega_2-\omega_1)/m\omega_o^2 = R(f_2-f_1)/2\pi f_1^2 \qquad (3\text{-}2)$$

$$C_2 = 1/R(\omega_2-\omega_1) = 1/2\pi R(f_2-f_1)\ , \qquad (3\text{-}3)$$

where R is the terminating resistance (both source and load), f_2 is the upper cutoff frequency, f_1 is the lower cutoff frequency, $f_o = (f_1 f_2)^{1/2}$ is the center frequency, and $m = f_1/f_2$.

3. The Three-Element Shunt II Bandpass Filter Section

The three-element shunt II bandpass filter section is shown in Fig. 3.2.

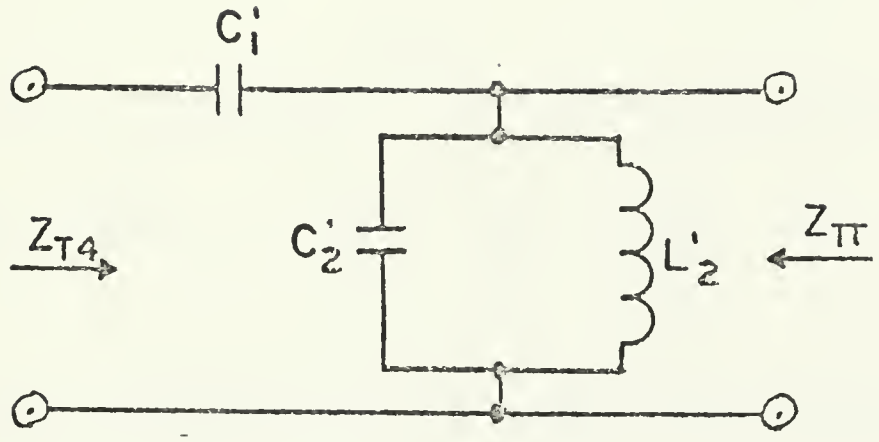

Figure 3.2. 3-Element Shunt II Bandpass Filter Section

Element values for this filter section are given by:

$$C_1' = (1+m)(\omega_2-\omega_1)/R\omega_o^2(1-m) = (f_1+f_2)/2\pi Rf_1f_2 \qquad (3\text{-}4)$$

$$C_2' = m/R(\omega_2-\omega_1) = f_1/2\pi Rf_2(f_2-f_1) \qquad (3\text{-}5)$$

$$L_2' = R(\omega_2-\omega_1)/\omega_o^2 = R(f_2-f_1)/2\pi f_1f_2 \ , \qquad (3\text{-}6)$$

where the quantities R, f_2, f_1, f_o, and m are as defined in the previous section.

4. Combination of Filter Sections for Inductor Simulation

Two three-element shunt I sections may be combined to form a pi section as shown in Fig. 3.3. This pi section is suitable for simulation of all the inductances using the "dual" Riordan gyrator circuit to produce the inductive pi network.

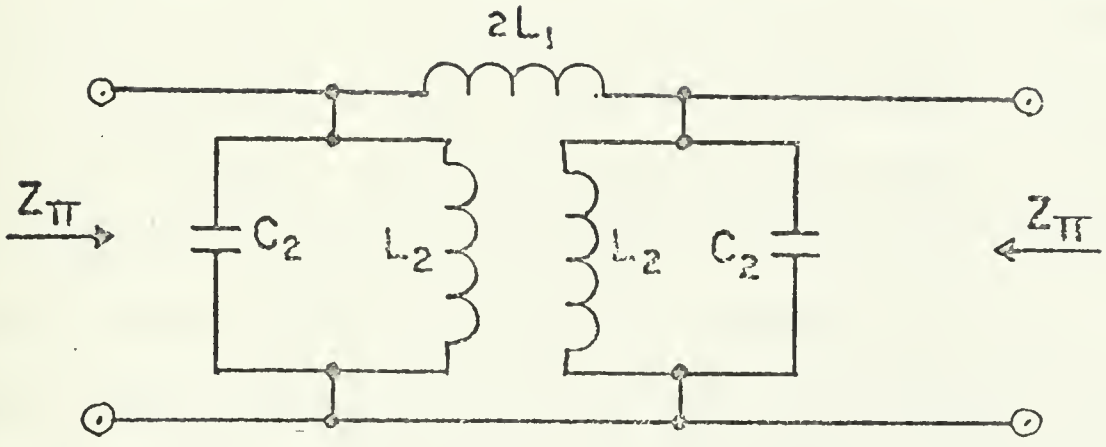

Figure 3.3. 3-Element Shunt I Pi Section

Two three-element shunt II sections may be combined to form a pi section as shown in Fig. 3.4.

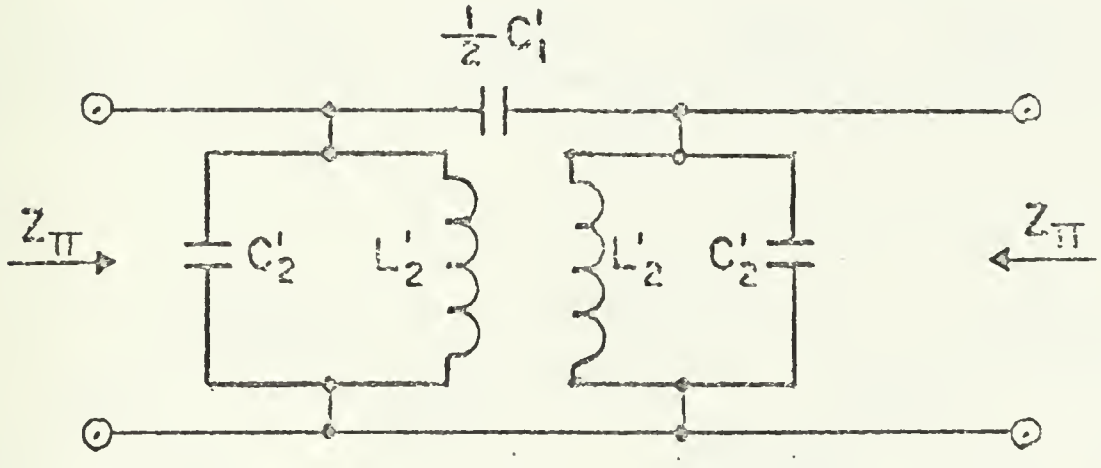

Figure 3.4. 3-Element Shunt II Pi Section

Each of the grounded inductors in this pi section may be simulated using a single Riordan gyrator.

A composite bandpass filter could then be constructed by combining a number of the pi sections shown in Figs. 3.3 and 3.4, depending on the amount of attenuation desired outside the passband. Of course, the total number of components (and hence the number of gyrators) required for a composite filter is less than the sum of the components in the individual filter sections due to series and parallel combination of components. To illustrate the process of building a composite filter, Fig. 3.5 shows how two shunt I pi sections

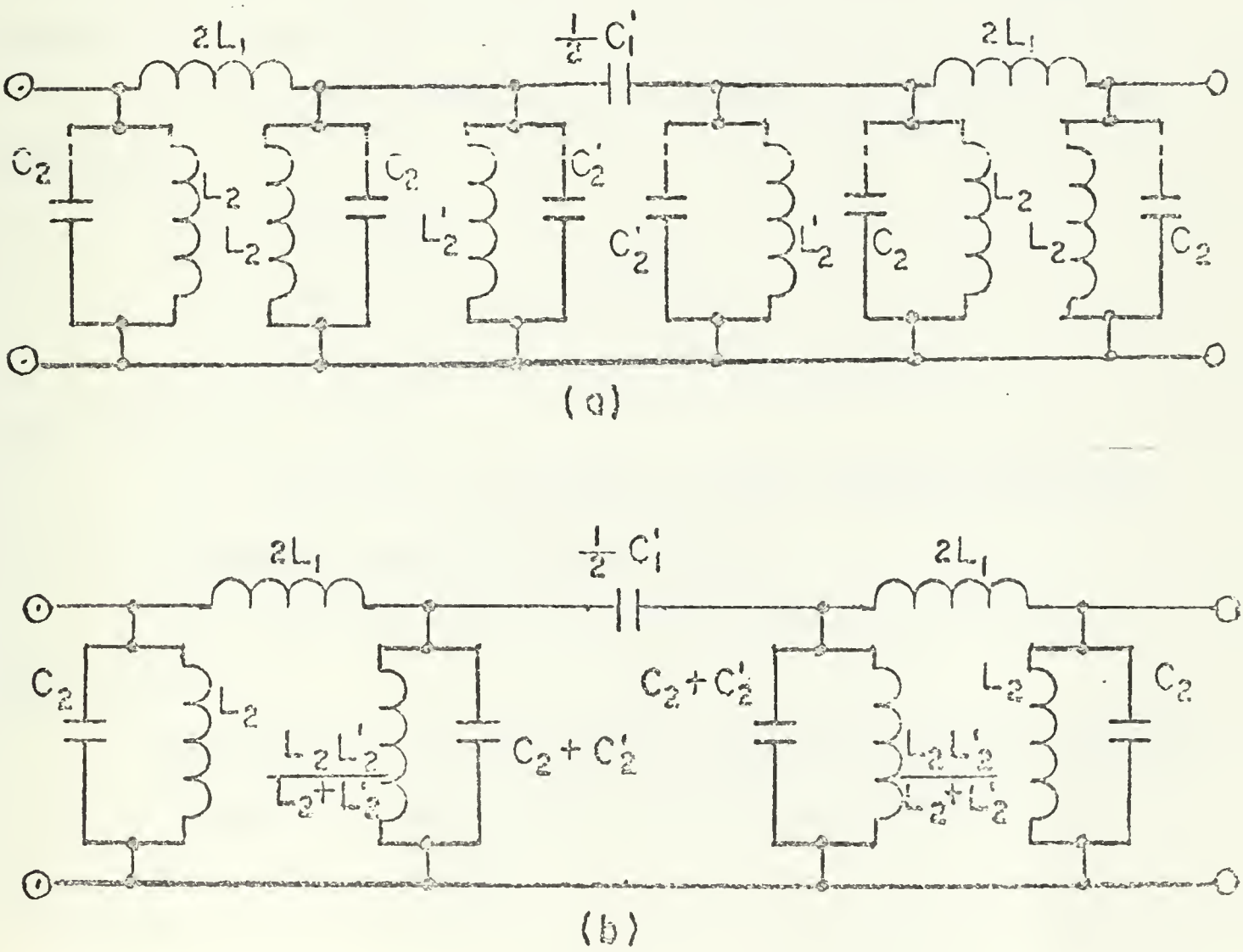

Figure 3.5. Formation of a Composite Bandpass Filter

and one shunt II pi section can be combined to form a composite bandpass filter. The filter shown in Fig. 3.5 is in the proper form for inductance simulation, and could be constructed using two "dual" Riordan gyrator circuits to simulate the two inductive pi networks.

B. EXPERIMENTAL DESIGN AND CONSTRUCTION OF THE FILTER.

1. Design Criteria

It was decided to construct a low-frequency bandpass filter such as might be used with a teletype terminal set. The two image-parameter filter sections discussed in the previous section were chosen as the basic filter building blocks. The specifications for the filter were as follows:

a. Use two shunt II pi sections and one shunt I pi section.

b. $f_o = 700$ Hz

c. $f_1 = 625$ Hz, $f_2 = 775$ Hz

d. Use equal source and load resistances ($R_S = R_L = R = 10$ KΩ).

e. Standardize component values wherever possible.

2. Prototype Experimental Circuit

The three pi sections were connected as shown in Fig. 3.6.

3. Calculation of Component Values for Prototype Circuit

Component values for the shunt I pi section in Fig. 3.6(a) are as follows:

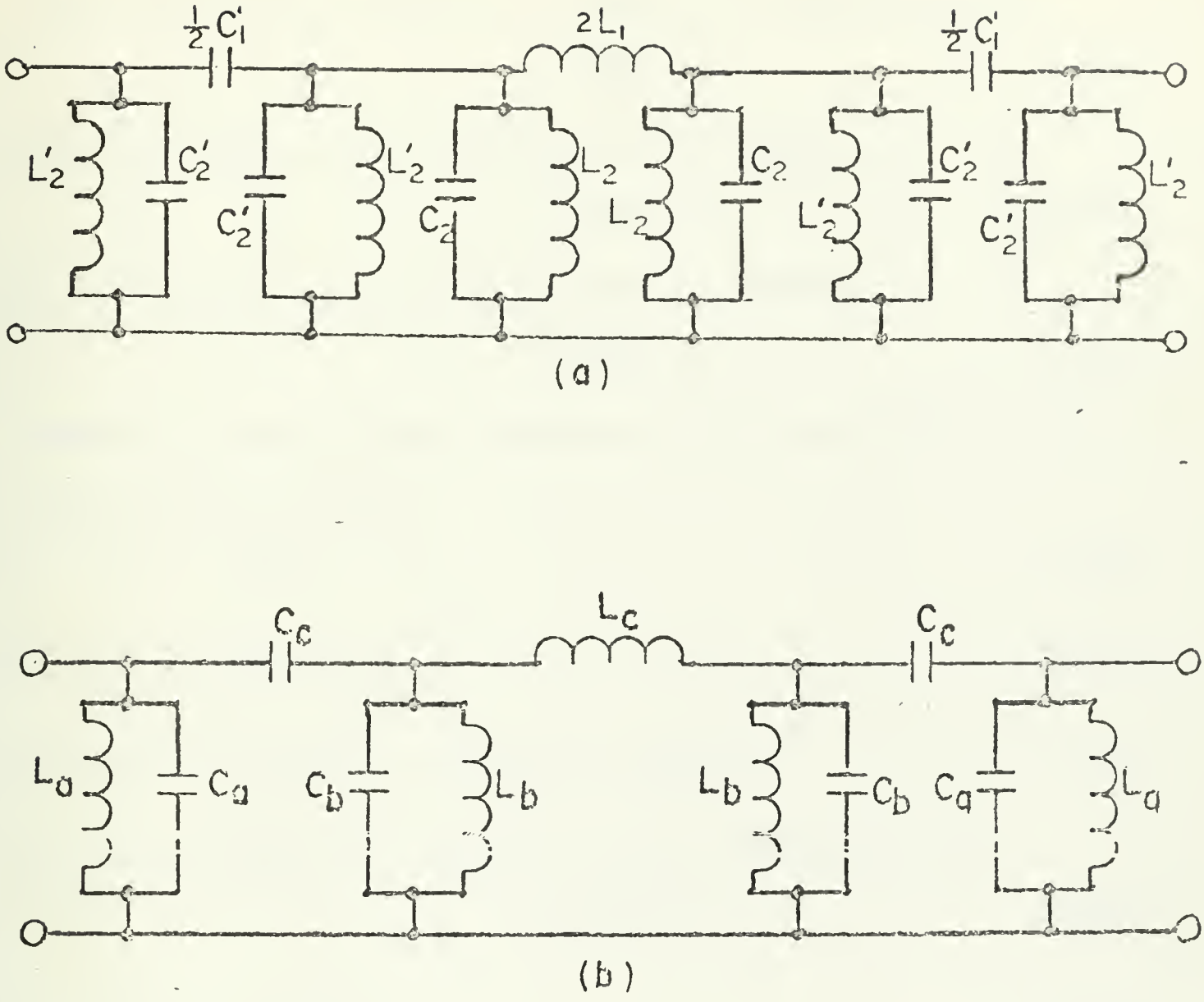

Figure 3.6. Prototype Bandpass Filter Circuit

$$2L_1 = 2R/2\pi(f_1+f_2) = 2\times10^4/2\pi(625+775) = 2.2736 \text{ H} \qquad (3\text{-}7)$$

$$L_2 = R(f_2-f_1)/2\pi f_1^2 = 10^4(775-625)/2\pi(625)^2 = .61116 \text{ H} \qquad (3\text{-}8)$$

$$C_2 = 1/2\pi R(f_2-f_1) = 1/2\pi\times10^4(775-625) = .10610 \text{ uF.} \qquad (3\text{-}9)$$

Component values for the shunt II pi sections in Fig. 3.6(a) are as follows:

$$C_1'/2=(1/2)(f_1+f_2)/2\pi Rf_1f_2 = .5(625+775)/2\pi x10^4 x625x775$$

$$= .02300 \text{ uF} \qquad (3\text{-}10)$$

$$C_2' = f_1/2\pi Rf_2(f_2-f_1) = 625/2\pi x10^4 x775(775-625)$$

$$= .085567 \text{ uF} \qquad (3\text{-}11)$$

$$L_2' = R(f_2-f_1)/2\pi f_1f_2 = 10^4(775-625)/2\pi x775x625$$

$$= .49287 \text{ H} . \qquad (3\text{-}12)$$

Component values for the combined circuit as shown in Fig. 3.6(b) are as follows:

$$L_a = L_2' = .49287 \text{ H} \qquad (3\text{-}13)$$

$$C_a = C_2' = .085567 \text{ uF} \qquad (3\text{-}14)$$

$$C_b = C_2+C_2' = .10610 + .085567 = .19167 \text{ uF} \qquad (3\text{-}15)$$

$$L_b = L_2L_2'/(L_2+L_2') = (.49287)(.61116)/(.49287+.61116)$$

$$= .27284 \text{ H} \qquad (3\text{-}16)$$

$$L_c = 2L_1 = 2.2736 \text{ H} \qquad (3\text{-}17)$$

$$C_c = C_1'/2 = .02300 \text{ uF} . \qquad (3\text{-}18)$$

4. Impedance Transformation to Equalize Capacitance Values

In order to make the capacitances in the shunt arm of each of the two capacitive pi networks equal, the filter circuit was bisected in the middle of L_c and then the impedance transformation process was carried out as indicated in Fig. 3.7.

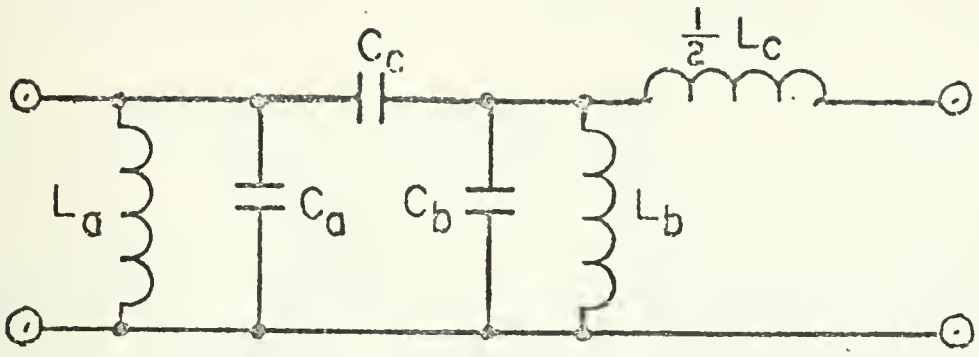

(a)

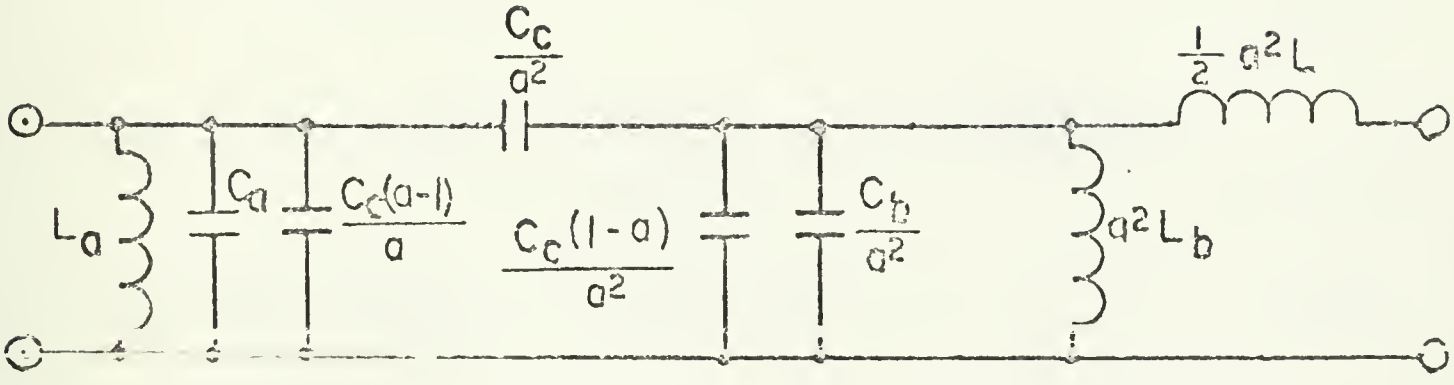

(b)

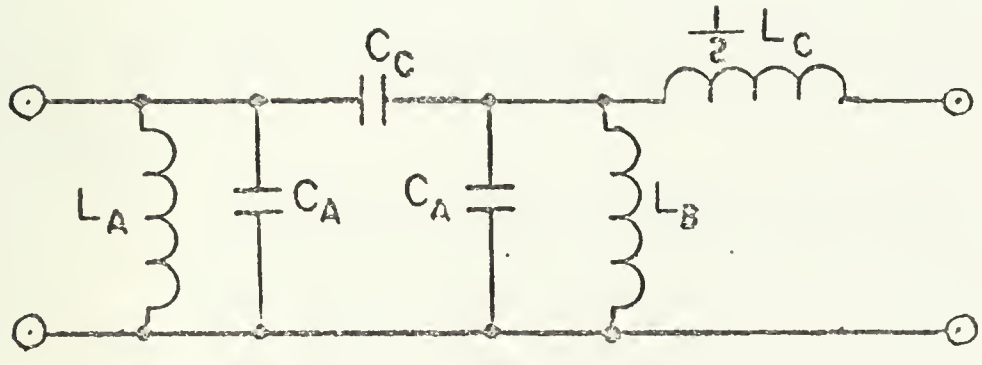

(c)

Figure 3.7. Impedance Transformation Process.

Calculations for the transformation are as follows:

$$C_a+C_c\left(\frac{a-1}{a^2}\right) = C_c\left(\frac{1-a}{a^2}\right) + \frac{C_b}{a^2} \tag{3-19}$$

$$C_a+C_c = \frac{C_c+C_b}{a^2} \tag{3-20}$$

$$\left[\frac{C_c+C_b}{C_a+C_c}\right]^{1/2} = \left[\frac{.02300+.19167}{.02300+.085567}\right]^{1/2} = 1.4062 \ . \tag{3-21}$$

Therefore the component values for the transformed circuit in Fig. 3.7(b) are as follows:

$$L_A = L_a = .49287 \text{ H} \tag{3-22}$$

$$C_A = C_a + C_c\left(\frac{a-1}{a}\right) = .085567 + .02300\left(\frac{1.4062-1.0}{1.4062}\right)$$

$$= .092210 \text{ uF} \tag{3-23}$$

$$C_C = \frac{C_c}{a^2} = \frac{.02300}{(1.4062)^2} = .016356 \text{ uF} \tag{3-24}$$

$$L_B = a^2L_b = (1.4062)^2 x .27284 = .53949 \text{ H} \tag{3-25}$$

$$L_C/2 = a^2L_c/2 = .5(1.4062)^2 x 2.2736 = 2.2478 \text{ H} \ . \tag{3-26}$$

The final circuit which was constructed is as shown in Fig. 3.8. Capacitances are in uF and inductances in Henrys.

5. Calculation of Gyrator Parameters

One Riordan gyrator circuit as shown in Fig. 3.9 was used to simulate each of the inductors L_1, L_4. The 741 operational amplifiers used had a DC gain of over 100 dB and a cutoff frequency f_c of approximately 10 Hz. All of the

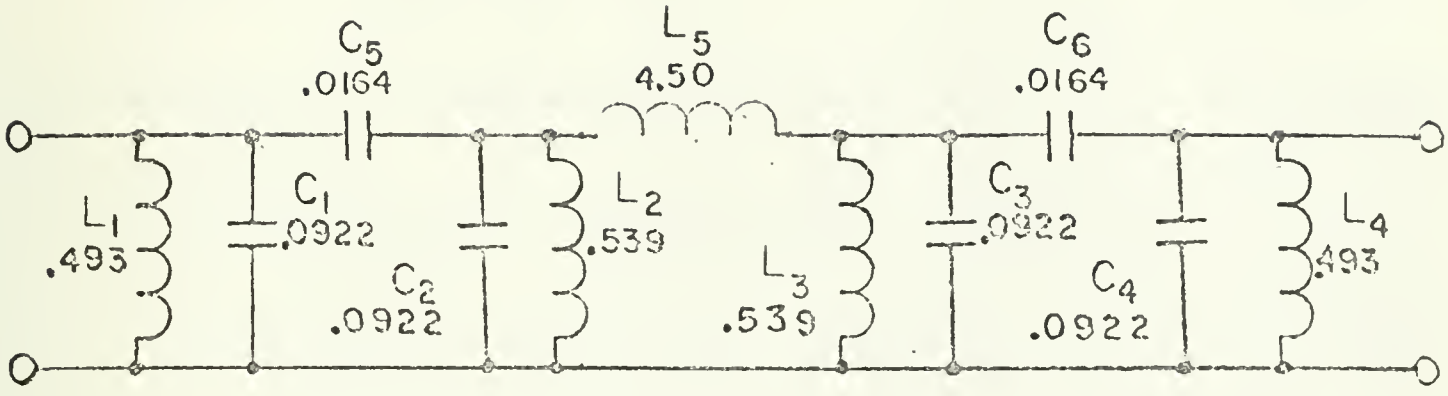

Figure 3.8. Final Form of Bandpass Filter Circuit

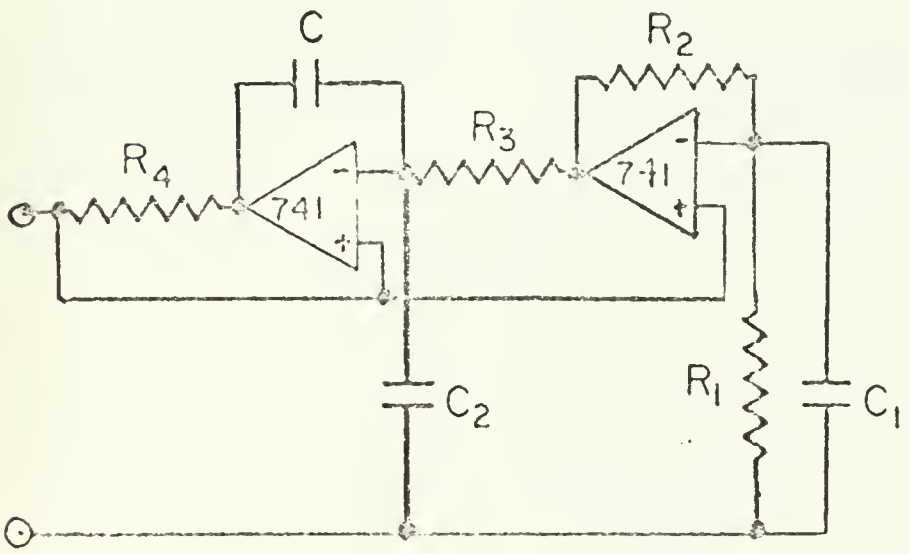

Figure 3.9. Riordan Gyrator Circuit

resistors in the gyrator were made equal at 10 KΩ. Other values are as computed below.

$$L_1 = L_4 = R_1R_3R_4C/R_2 = R^2C \tag{3-27}$$

$$C = L_1/R^2 = .49287/(10^4)^2 \doteq .00493\ \mu F \tag{3-28}$$

$$D = \omega(R_1C_1-R_3C_2) + a(\omega R_3C+1/\omega R_3C) - 4a\omega/\omega_c$$

$$\doteq \omega R(C_1-C_2) + a(\omega RC+1/\omega RC) - 4af/fc \doteq 0 \tag{3-29}$$

$$C_1-C_2 \doteq \frac{1}{\omega R}[4af/f_c-a(\omega RC+1/\omega RC)]$$

$$\doteq \frac{1}{2\pi x700x10^4}\,[4x10^{-5}x700/10$$

$$-10^{-5}(2\pi x700x10^4x5x10^{-9}$$

$$+ \frac{1}{2\pi x700x10^4x5x10^{-9}})]$$

$$\doteq 63\ pF \tag{3-30}$$

One "dual" Riordan gyrator circuit as shown in Fig. 3.10 was used to simulate the inductive pi network consisting of L_2, L_3, and L_5.

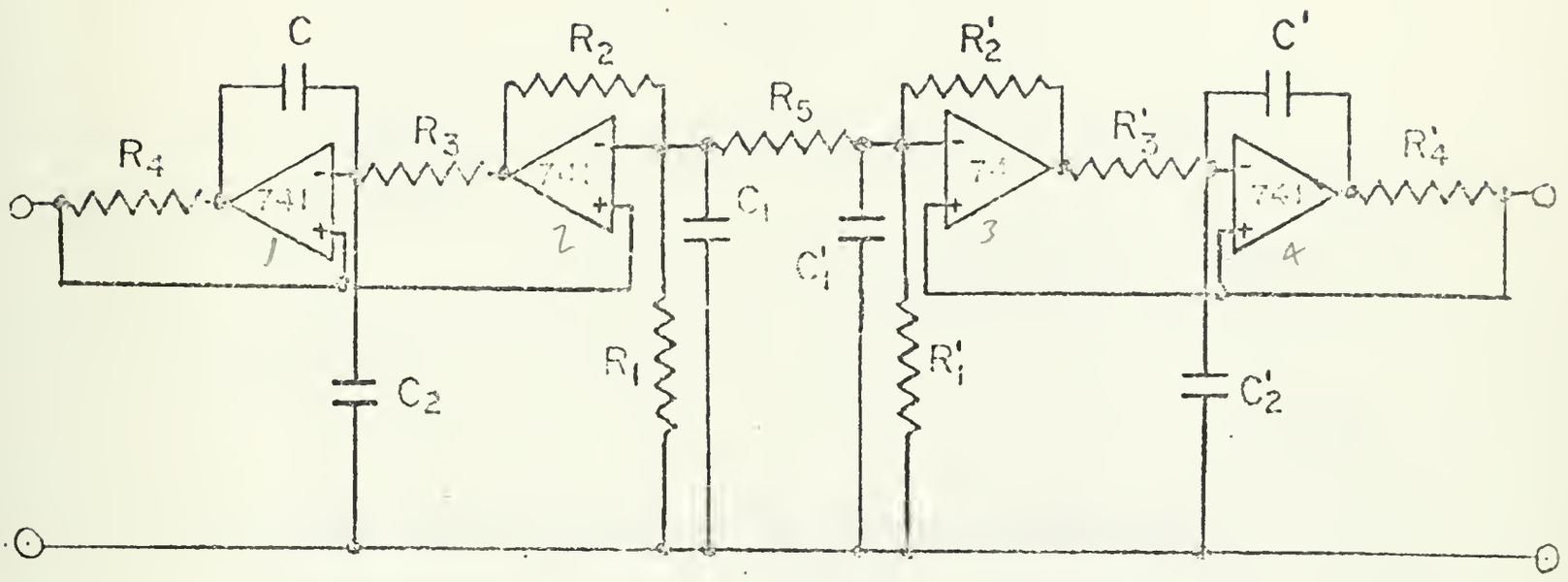

Figure 3.10. "Dual" Riordan Gyrator Circuit

Again, all resistors in the gyrator were made equal at 10?KΩ. Also, the primed capacitors were made equal to the unprimed capacitance values. Other values are as computed below.

$$L_2 = L_3 = R_1R_3R_4C/R_2 = R^2C \qquad (3\text{-}31)$$

$$C = L_2/R^2 = .53949/(10^4)^2 \doteq .00539 \text{ uF} \qquad (3\text{-}32)$$

$$L_5 = R_3R_4R_5C/R_2 = RR_5C \qquad (3\text{-}33)$$

$$R_5 = L_5/RC = 4.4956/10^4 \times 5.39\times10^{-9} = 82.5 \text{ K}\Omega \qquad (3\text{-}34)$$

$$D = \omega(R_1C_1-R_3C_2)+a(\omega R_3C+1/\omega R_3C)-4a\omega/\omega_c$$

$$= \omega R(C_1-C_2)+a(\omega RC+1/\omega RC)-4af/f_c \doteq 0 \qquad (3\text{-}35)$$

$$C_1 - C_2 \doteq \frac{1}{\omega R}[4af/f_c - a(\omega RC + 1/\omega RC)]$$

$$= \frac{a}{\omega R}[4f/f_c - (\omega RC + 1/\omega RC)]$$

$$\doteq \frac{10^{-5}}{2\pi \times 700 \times 10^4}\left[4 \times 700/10 - \left(2\pi \times 700 \times 10^4 \times 5.39 \times 10^{-9} + \frac{1}{2\pi \times 700 \times 10^4 \times 5.39 \times 10^{-9}}\right)\right]$$

$$\doteq 63 \text{ pF}$$

(3-36)

6. Experimental Setup and Measurement Techniques

All components used to construct the filter were within 1% tolerance of computed values. Nevertheless, to obtain the proper frequency response from the filter, it was necessary to tune the filter. This was accomplished by making the resistor R_4 in each gyrator a combination of fixed resistance and a small trimmer potentiometer. Each of the four parallel resonant LC circuits was then decoupled temporarily from the rest of the circuit and tuned to its proper resonant frequency as determined from the previously computed values of L and C for the exact circuit.

After tuning each tank circuit, the filter was then reassembled, and the setup shown in Fig. 3.11 was used to make frequency response measurements on the circuit.

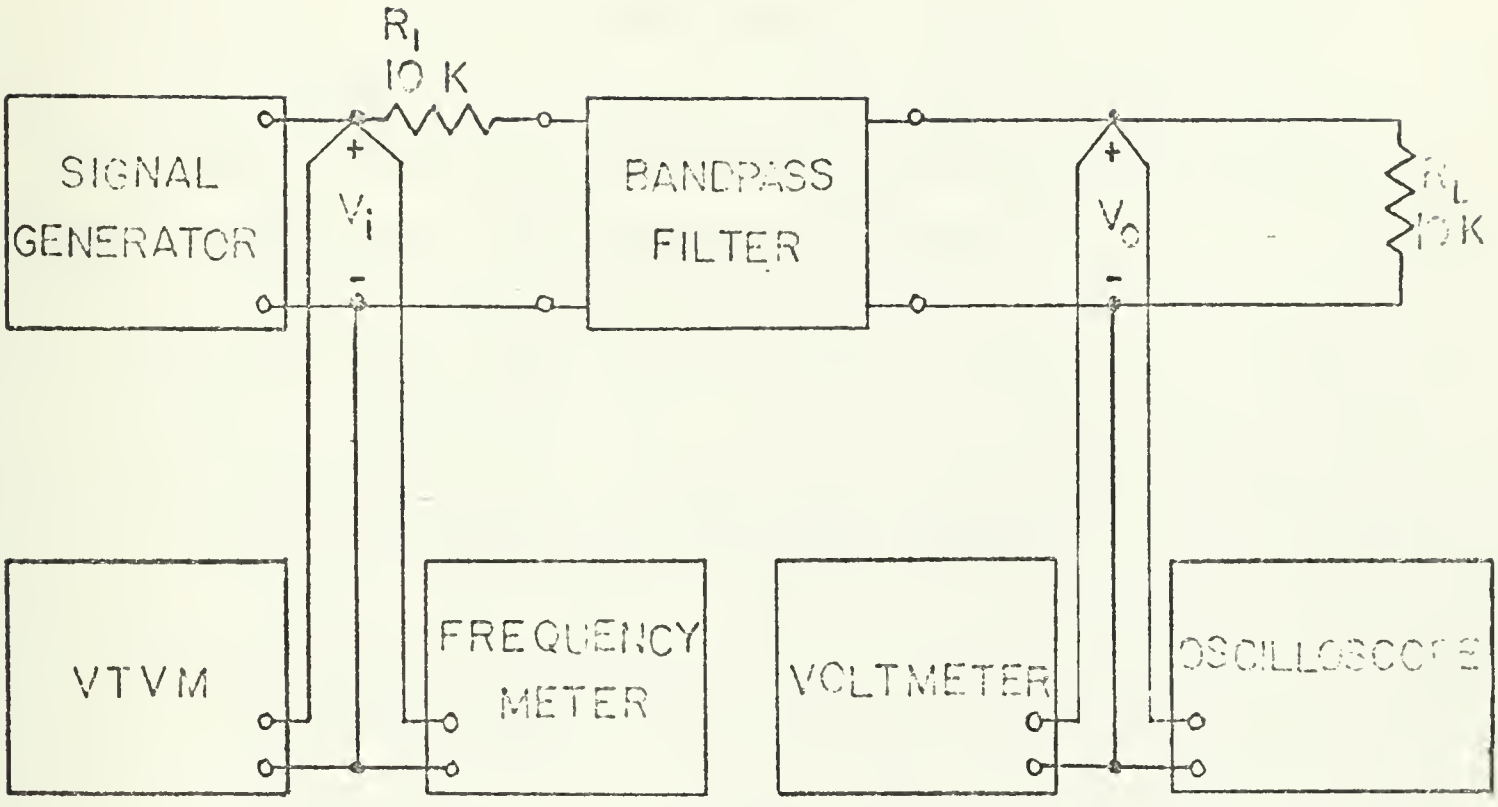

Figure 3.11. Test Setup

7. Experimental Data

a. Saturation Level

As the input from the signal generator was increased at midband frequency, the input and output of the filter were monitored for indications of saturation. The filter appeared to start into saturation at V_i = 2.83 volts rms. This corresponds to a maximum input power of

$$P_{max}=V_{max}^2/R_L=(2.83)^2/10^4=.8 \text{ mW}=-1.0 \text{ dBm} . \quad (3\text{-}37)$$

b. DC Power Consumption

Each of the operational amplifiers required a positive and a negative power supply voltage of $V_{DC}=\pm 18$ V. The power supply current I_{DC} was then measured for full-load (input at saturation level) and no-load (zero filter input) conditions, with results as follows:

(1) For $V_{in} = V_{sat} = 2.83$ V rms:

$$I_{DC} = 16.9 \text{ mA}$$

$$P_{DC} = 2V_{DC}I_{DC} = 2x18x.0169 = 608 \text{ mW}. \qquad (3\text{-}38)$$

(2) For $V_{in} = 0$:

$$I_{DC} = 16.2 \text{ mA}$$

$$P_{DC} = 2V_{DC}I_{DC} = 2x18x.0162 = 584 \text{ mW}. \qquad (3\text{-}39)$$

c. Frequency Response

The signal generator which was used as the filter input source had an output impedance of 50 ohms, which, in series with the 10 Kohm resistor R_1, presented a very close match to the 10 Kohm load resistor R_L. The effective representation of the signal generator in the test circuit is shown in Fig. 3.12.

Now the insertion loss of a filter is defined as

$$L_{dB} = 10 \log (P_{ob}/P_{oa}) , \qquad (3\text{-}40)$$

where P_{ob} is the output power at the load before filter

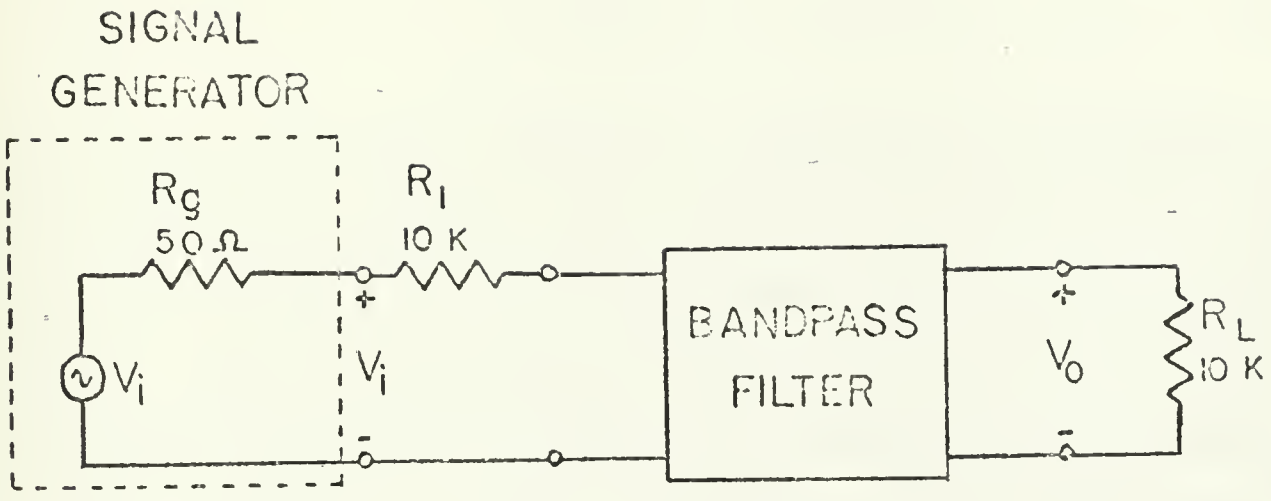

Figure 3.12. Test Circuit

insertion, and P_{oa} is the output power at the load after filter insertion. From Eq. (3-40) it follows that

$$L_{dB} = 10 \log[(V_{ob}^2/R_L)/(V_{oa}^2/R_L)] = 10 \log (V_{ob}^2/V_{oa}^2)$$

$$= 20 \log (V_{ob}/V_{oa}) = 20 \log[(V_{ob}/V_i)/(V_{oa}/V_i)]$$

$$= 20 \log\{[R_L/(R_L+R_1)]/(V_{oa}/V_i)\} = 20 \log[1/(2V_{oa}/V_i)]$$

$$= 20 \log (V_i/2V_{oa}). \qquad (3\text{-}41)$$

The input voltage V_i was kept constant at two volts throughout all frequency response measurements, therefore Eq. (3-41) becomes

$$L_{dB} = 20 \log (1/V_o) = -20 \log V_o. \qquad (3\text{-}42)$$

Frequency response measurements were taken with the gyrator Q-adjusting capacitors C_1 and C_2 at three different sets of values: 1) $C_1 = 68$ pF, $C_2 = 0$; 2) $C_1 = C_2 = 0$; and 3) $C_1 = 0$, $C_2 = 33$ pF. Under the first set of conditions, with C_1 near the theoretically required value of 63 pF, the maximum value of output in the passband was only 90% of the expected value, representing a loss of about one dB. This was probably attributed somewhat to losses in the capacitors, but more probably to slight variations in the filter component values and/or a slight mismatch between source and load impedances. Under the second set of conditions, with both C_1 and C_2 zero, the maximum output in the passband approached 97% of the expected value, and under the third set of conditions, with C_1 at zero and C_2 (the Q-boosting capacitor) at 33 pF, the maximum output rose to 98% of the expected value.

The theoretical response of the filter was computed aforehand using the LISA 360A linear systems analysis computer program. The results appear with the experimental data in tabular form in Table I, and in graphical form in Figs. 3.13-3.16. Complete measurements were made only for conditions (2) and (3) as defined in the preceding paragraph.

TABLE I

FILTER FREQUENCY RESPONSE

Freq (Hz)	Expected Results (LISA)		Experimental Results (C_1=C_2=0)		Experimental Results (C_1=0, C_2=33 pF)	
	V_o (mV)	L_{dB}	V_o (m_V)	L_{dB}	V_o (mV)	L_{dB}
500	3.94	48.1	3.83	48.3	3.83	48.3
510	5.21	45.7	5.05	45.9	4.95	46.1
520	6.97	43.1	6.78	43.4	6.75	43.4
530	9.44	40.5	9.25	40.7	9.14	40.8
540	13.0	37.7	12.5	38.1	12.6	38.0
550	18.1	34.8	17.5	35.1	17.6	35.1
560	25.8	31.8	25.2	32.0	25.0	32.0
570	37.6	28.5	36.3	28.8	35.4	29.0
580	45.4	25.0	54.7	25.2	55.2	25.2
590	87.5	21.2	85.0	21.4	85.2	21.4
600	141	17.0	137	17.3	134	17.5
605	182	14.8	181	14.8	177	15.0
610	238	12.5	236	12.5	229	12.8
615	314	10.1	305	10.3	308	10.2
620	415	7.68	398	8.00	398	8.00
625	543	5.33	530	5.51	523	5.63
630	690	3.26	659	3.62	659	3.62
635	828	1.68	778	2.18	789	2.06
640	926	0.70	865	1.26	879	1.12
645	978	0.22	915	0.77	940	0.54
650	997	0.05	942	0.52	961	0.35
655	1002	0.00	951	0.44	968	0.28
660	1002	0.00	958	0.37	972	0.25
665	1002	0.00	960	0.35	974	0.23
670	1002	0.00	963	0.33	976	0.21
675	1002	0.00	964	0.32	977	0.20
680	1002	0.00	965	0.31	978	0.19
685	1002	0.00	966	0.30	978	0.18
690	1002	0.00	967	0.29	978	0.18
695	1002	0.00	968	0.28	978	0.18
700	1002	0.00	968	0.28	978	0.18
705	1002	0.00	968	0.28	978	0.18
710	1002	0.00	968	0.28	978	0.18
715	1002	0.00	968	0.28	978	0.18
720	1002	0.00	967	0.29	980	0.18
725	1002	0.00	966	0.30	979	0.18
730	1002	0.00	965	0.31	979	0.18

TABLE I--Continued

Freq (Hz)	Expected Results (LISA)		Experimental Results (C_1=C_2=0)		Experimental Results (C_1=0, C_2=33 pF)	
	V_o (mV)	L_{dB}	V_o (mV)	L_{dB}	V_o (mV)	L_{dB}
735	1002	0.00	963	0.33	978	0.19
740	1002	0.02	958	0.37	975	0.22
745	993	0.08	943	0.51	968	0.28
750	975	0.25	910	0.82	947	0.47
755	937	0.60	855	1.36	890	1.01
760	873	1.22	788	2.07	822	1.70
765	783	2.16	703	3.06	737	2.65
770	678	3.41	605	4.36	638	3.90
775	571	4.90	503	5.97	525	5.60
780	474	6.53	418	7.58	442	7.09
785	390	8.20	339	9.40	360	8.87
790	322	9.87	279	11.1	299	10.5
795	267	11.5	231	12.7	247	12.1
800	222	13.1	196	14.2	209	13.6
810	158	16.0	140	17.1	148	16.6
820	116	18.8	104	19.7	108	19.3
830	86.9	21.2	78.8	22.1	83.2	21.6
840	66.8	23.5	60.3	24.4	63.4	24.0
850	52.4	25.6	48.7	26.2	49.7	26.1
860	41.8	27.6	39.0	28.2	39.5	28.1
870	33.9	29.4	31.7	30.0	32.0	29.9
880	27.9	31.1	26.0	31.7	26.2	31.6
890	23.2	32.7	21.7	33.3	21.8	33.2
900	19.5	34.2	18.3	34.8	18.5	34.7
910	16.6	35.6	15.5	36.2	15.6	36.1
920	14.2	37.0	13.4	37.5	13.4	37.5
930	12.2	38.3	11.5	38.8	11.6	38.7
940	10.6	39.5	9.95	40.0	10.1	39.9
950	9.30	40.6	8.75	41.2	8.83	41.1
960	8.19	41.7	7.80	42.2	7.77	42.2
970	725	42.8	6.82	43.3	6.84	43.3
980	6.44	43.8	6.07	44.3	6.12	44.3
990	5.76	44.8	5.42	45.3	5.49	45.2
1000	5.16	45.7	4.88	46.2	4.90	46.2

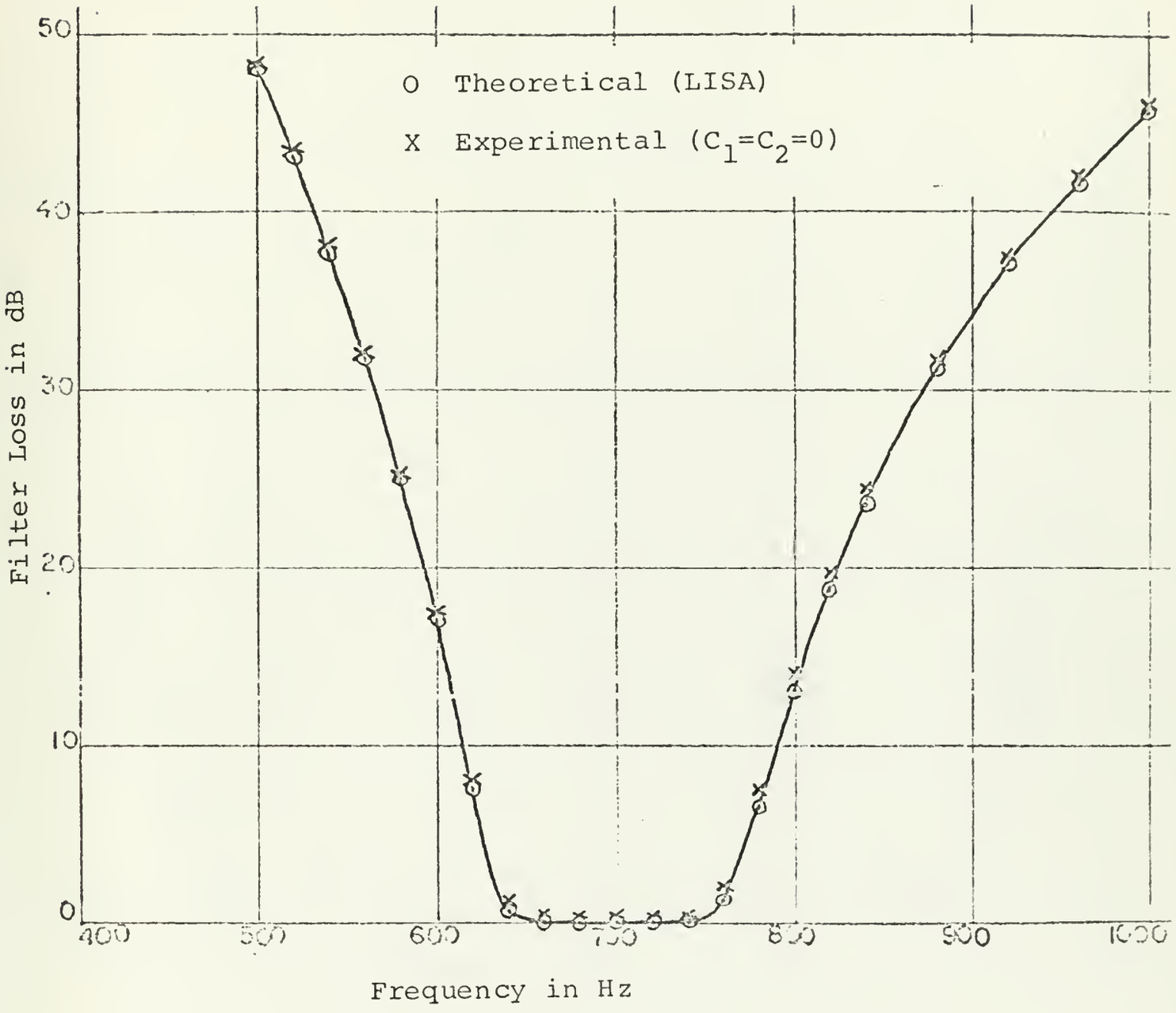

Figure 3.13. Overall Frequency Response of Filter

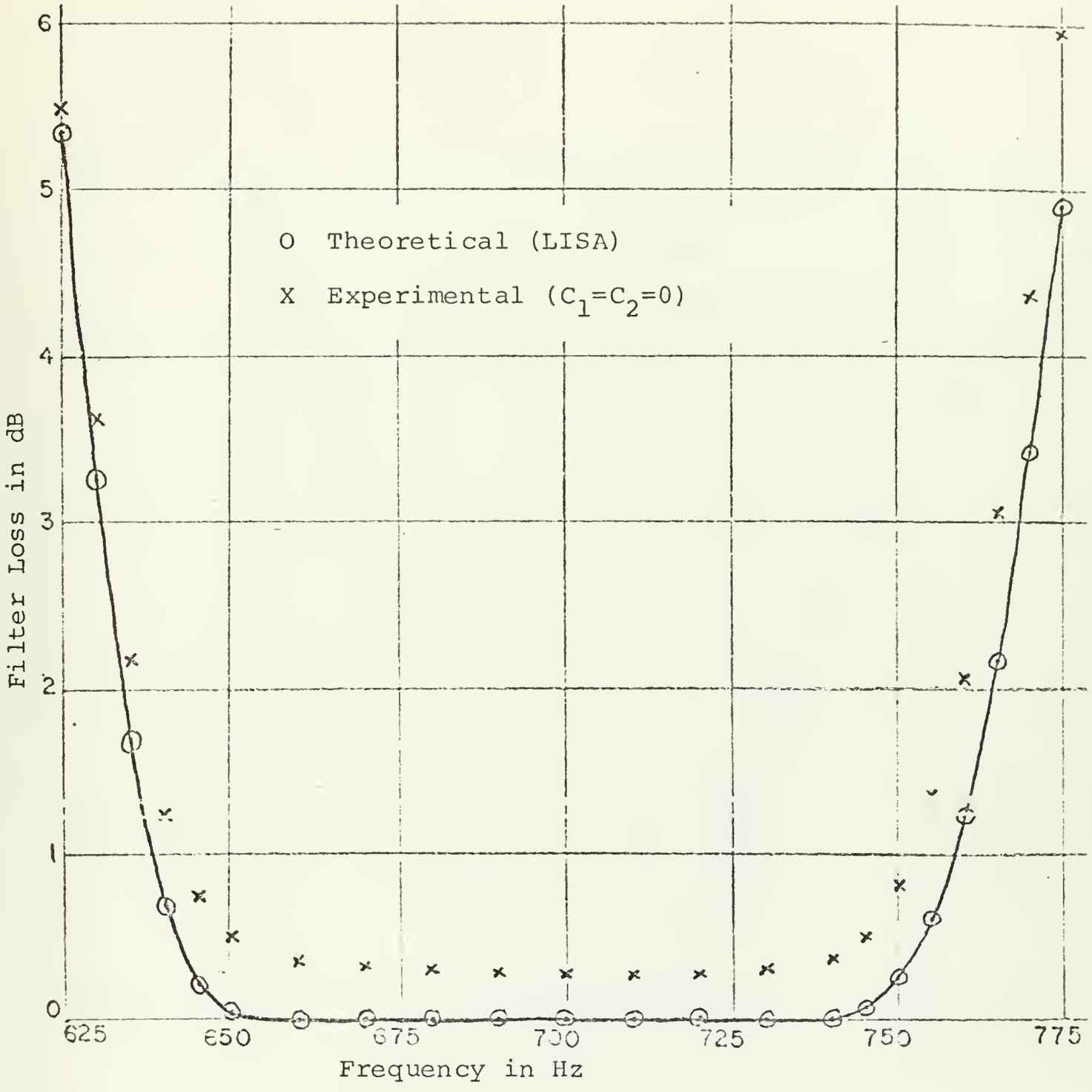

Figure 3.14. Passband Frequency Response of Filter

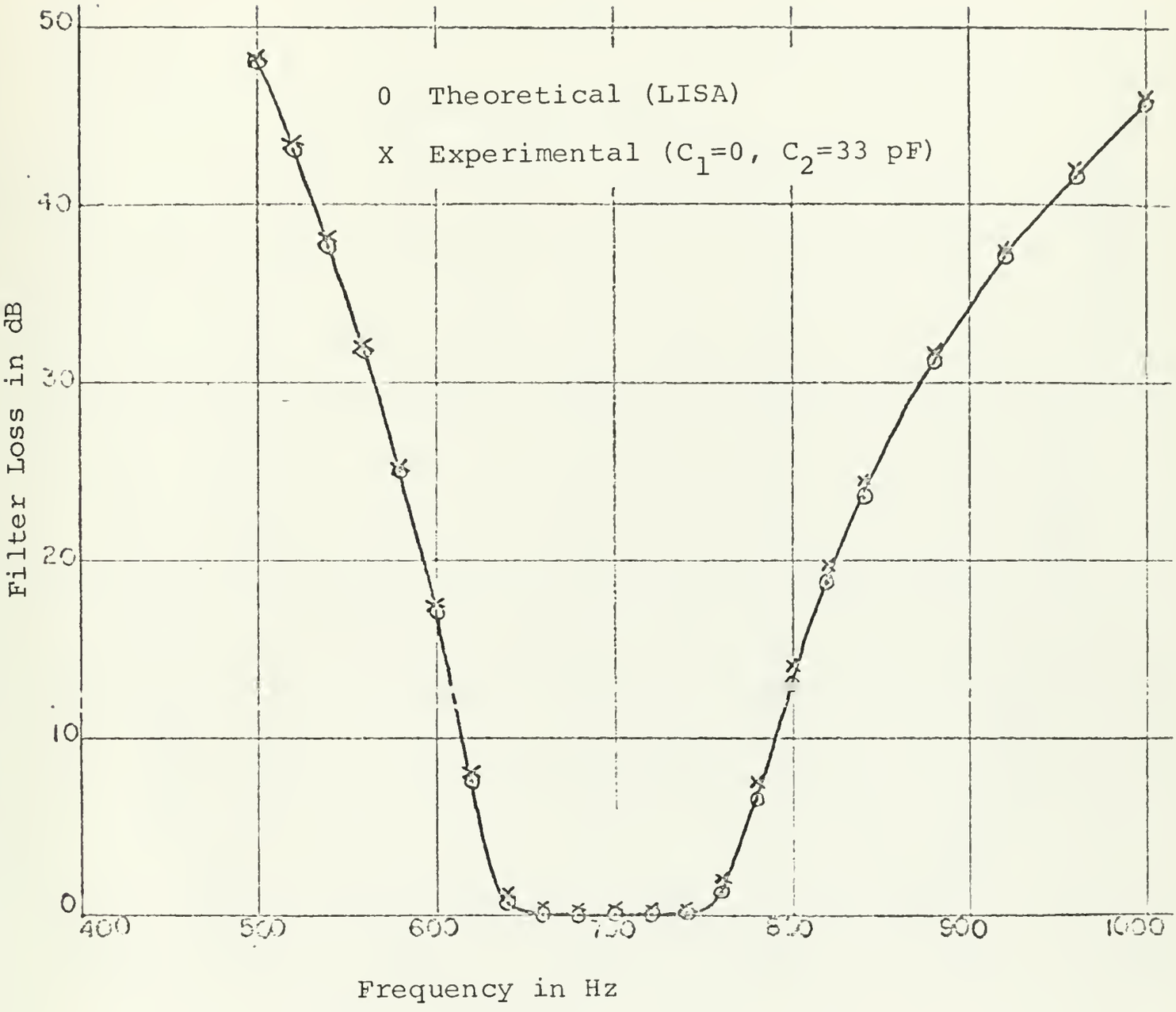

Figure 3.15. Overall Frequency Response of Filter

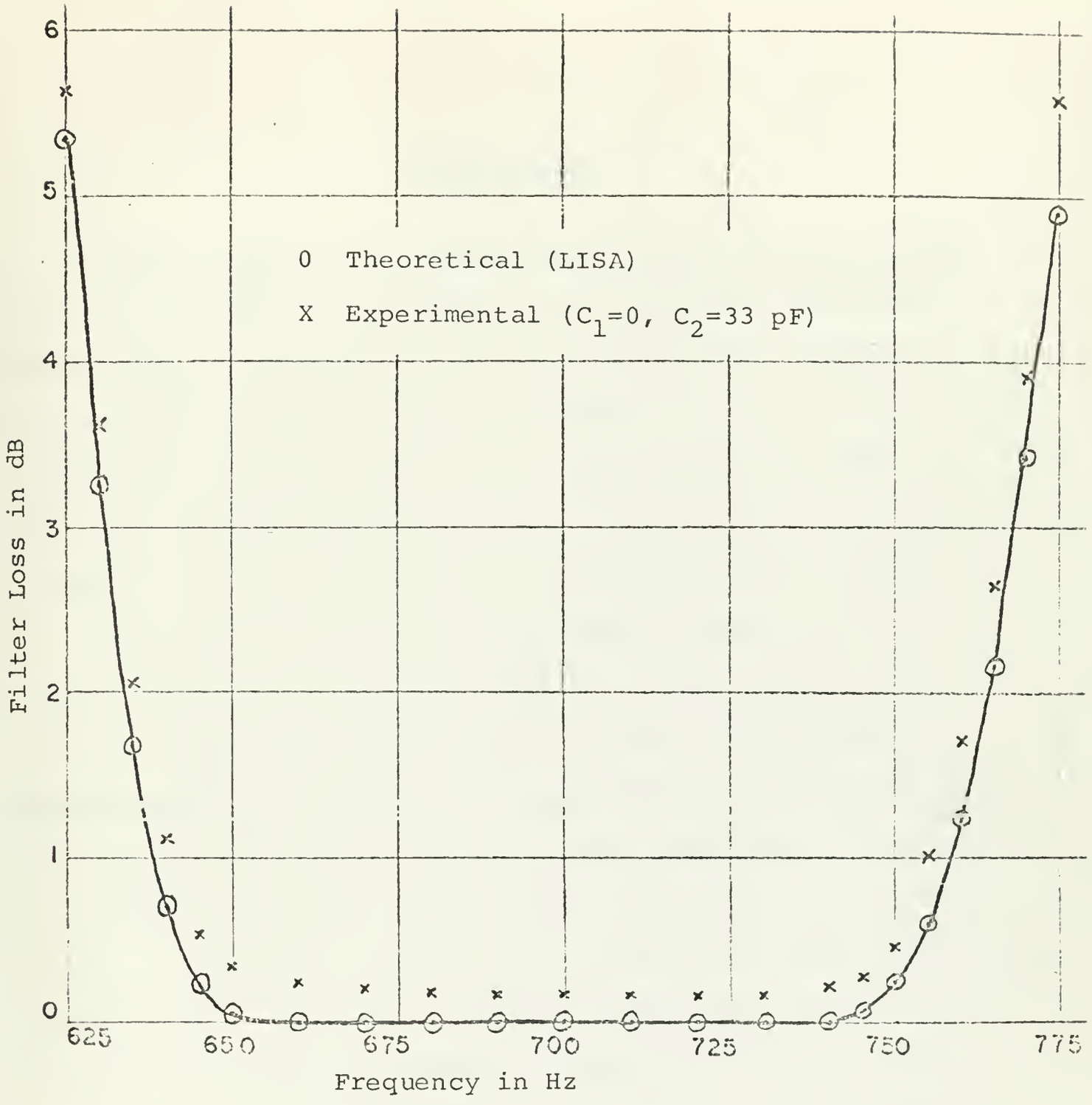

Figure 3.16. Passband Frequency Response of Filter

IV. CONCLUSIONS

Theory predicts that high-quality single grounded inductors and inductive pi networks can be produced using the Riordan gyrator circuits, and that inductorless filters constructed with these circuits should have sensitivities comparable to normal LC filters. Experimentation such as that done by Orchard and Sheahan [5] and that which was performed in this thesis has indeed validated these theories.

Hence, filter circuits which require large values of inductance may be produced using the Riordan gyrator to simulate these inductances with a considerable savings in physical size and improvement in Q-factor. The Riordan gyrators constructed for this thesis were made using off-the-shelf operational amplifiers and discrete resistors and capacitors, however the Riordan circuit could easily be totally integrated, provided the inductance-forming capacitor were not too large. In the latter case, an external capacitor could be used.

Because the size of physical inductors used in higher frequency applications becomes relatively small, for economic reasons then the gyrator's effectiveness for inductance simulation is probably limited to frequencies below about 100 kHz, with the greatest advantage being realized at very low frequencies. There may be a possible advantage in using gyrator-simulated inductances at high frequencies, though,

in that unlike a physical inductor, there is no electromagnetic field associated with one produced by a gyrator.

Finally, because the Riordan gyrator circuits may be used only to simulate either a grounded inductor or a pi network of inductors, their use is restricted to highpass and bandpass filter circuits. The problem of simulating a single high-quality floating inductor is as yet unresolved, and therefore the construction of an inductorless lowpass filter circuit using the gyrator is a problem for future study.

LIST OF REFERENCES

1. Tellegen, B. D. H., "The Gyrator, a New Network Element," Philips Research Report, v. 3, No. 2, p. 81-101, April 1948.

2. Kulesz, J. J., Jr., A Study of Gyrator Circuits, MS thesis, United States Naval Postgraduate School, Monterey, 1969.

3. Riordan, R. H. S., "Simulated Inductors Using Differential Amplifiers," Electronics Letters, v. 3, No. 2, p. 50-51, February 1967.

4. Antoniou, A., "Stability Properties of Some Gyrator Circuits," Electronics Letters, v. 4, No. 2, p. 510-512, November 1968.

5. Orchard, H. J., and Sheahan, D. F., "Inductorless Bandpass Filters," IEEE Journal of Solid-State Circuits, v. SC-5, No. 3, p. 108-118, June 1970.

6. Czarski-Popiel, T., "RC-Active Synthesis Using Positive Immittance Converters," Electronics Letters, v. 3, No. 8, p. 381-382, August 1967.

7. Norton, E. L., Transformer Band Filters, U.S. Patent 1,681,554, 21 August 1928.

8. Shea, T. E., Transmission Networks and Wave Filters, p. 325-332, D. Van Nostrand, 1929.

9. Reference Data for Radio Engineers, p. 7.5 - 7.14, Howard W. Sams & Co., Inc., 1969.

INITIAL DISTRIBUTION LIST

		No. Copies
1.	Defense Documentation Center Cameron Station Alexandria, Virginia 22314	2
2.	Library, Code 0212 Naval Postgraduate School Monterey, California 93940	2
3.	Professor S. R. Parker, Code 52 Px Department of Electrical Engineering Naval Postgraduate School Monterey, California 93940	1
4.	LT Robert E. Mollet, USN 374-A Bergin Dr. Monterey, California 93940	1

DOCUMENT CONTROL DATA - R & D

(Security classification of title, body of abstract and indexing annotation must be entered when the overall report is classified)

1 ORIGINATING ACTIVITY (Corporate author)
Naval Postgraduate School
Monterey, California 93940

2a. REPORT SECURITY CLASSIFICATION
Unclassified

2b. GROUP

3 REPORT TITLE
INDUCTORLESS BANDPASS FILTER REALIZATION USING THE RIORDAN GYRATOR

4 DESCRIPTIVE NOTES (Type of report and inclusive dates)
Master's Thesis; September, 1971

5 AUTHOR(S) (First name, middle initial, last name)
Robert Edward Mollet
Lieutenant, United States Navy

6 REPORT DATE	7a. TOTAL NO. OF PAGES	7b. NO. OF REFS
September 1971	80	9

8a. CONTRACT OR GRANT NO.	9a. ORIGINATOR'S REPORT NUMBER(S)
b. PROJECT NO.	
c.	9b. OTHER REPORT NO(S) (Any other numbers that may be assigned this report)
d.	

10. DISTRIBUTION STATEMENT
Approved for public release; distribution unlimited.

11. SUPPLEMENTARY NOTES	12. SPONSORING MILITARY ACTIVITY
	Naval Postgraduate School Monterey, California 93940

13. ABSTRACT

Since the gyrator was introduced over twenty years ago, a considerable number of realizations of the gyrator circuit have appeared in the technical literature. This thesis is confined to the study of only one of these, namely the Riordan gyrator circuit. The scope of the thesis is to analyze the parameters of the Riordan gyrator and those of an inductor simulated using it, and to investigate the use of simulated inductors in electric filter networks. To illustrate and support the theory surrounding the Riordan gyrator, an inductorless bandpass filter is designed, constructed, and tested.

KEY WORDS	LINK A		LINK B		LINK C	
	ROLE	WT	ROLE	WT	ROLE	WT
gyrator						
inductorless filter						